

Design and evaluation of BOOGIE: a collector for the analysis of cloud composition and processes

Mickael Vaitilingom^{1,2*}, Christophe Bernard³, Mickaël Ribeiro¹, Christophe Verhaege^{1,4}, Christophe Gourbeyre¹, Christophe Berthod⁵, Angelica Bianco¹, Laurent Deguillaume^{1,3*}

¹ Laboratoire de Météorologie Physique, UMR 6016, CNRS, Université Clermont Auvergne, 63178 Aubière, France.

² Laboratoire de Recherche en Géosciences et Énergies, EA 4539, Université des Antilles, 97110 Pointe-à-Pitre, France.

³ Observatoire de Physique du Globe de Clermont-Ferrand, UAR 833, CNRS, Université Clermont Auvergne, 63178 Aubière, France.

⁴ Institut Universitaire de Technologie Clermont Auvergne - site de Montluçon, Université Clermont Auvergne, 03100 Montluçon, France.

⁵ Division Technique de l'Institut National des Sciences de l'Univers, UAR 855, CNRS, 91190 Gif-sur-Yvette, France.

Correspondence to: Laurent Deguillaume (laurent.deguillaume@uca.fr) and Mickael Vaitilingom (mickael.vaitilingom@univ-antilles.fr)

Abstract. In situ cloud studies are fundamental to study the variability in cloud chemical and biological composition as a function of environmental conditions and assess their potential for transforming chemical compounds. To achieve this objective, cloud water collectors have been developed in recent decades to recover water from clouds and fogs using different designs and collection methods. In this study, a new active ground-based cloud collector was developed and tested for sampling cloud water to assess the cloud microbiology and chemistry. This new instrument, BOOGIE, is a mobile sampler for cloud water collection easy to operate with the objective of being cleanable and sterilisable, respecting chemical and microbial cloud integrity, and presenting an efficient collection rate of cloud water. Computational fluid dynamics simulations were performed to theoretically assess the capture of cloud droplets by this new sampler. A 50% collection efficiency cutoff of 12 μm has been estimated. The collector was deployed at Puy de Dôme station under cloudy conditions for evaluation. The water collection rates were measured at $100 \pm 53 \text{ mL h}^{-1}$ for a collection of 21 cloud events; considering the measured liquid water content, the sampling efficiency of this new collector has been estimated at $69.7 \pm 11\%$ over the same set of cloud events. BOOGIE was compared with other active cloud collectors commonly used by the scientific community (Cloud Water Sampler and Caltech Active Strand Cloud Collector version 2). The three samplers presented similar collection efficiencies (between 53% and 70% on average). The sampling process can affect the endogenous cloud water microflora, but the ATP/ADP ratio obtained from the samplers indicate that they are not stressful for the cloud microorganisms. The chemical composition of hydrogen peroxide, formaldehyde and major ions are similar between the collectors; a significant variability is observed for magnesium and potassium that are the less concentrate ions. The differences between collectors are the consequence of different designs, and the intrinsic homogeneity in the chemical composition within the cloud system.

Keywords: Cloud chemistry, monitoring, cloud water collector, chemical composition, biological composition.

44 **1 Introduction**

45 The chemical composition of clouds is highly complex because it results from various processes: (1) the mass
46 transfer of soluble compounds from the gas phase into cloud droplets, (2) dissolution of the cloud condensation
47 nuclei released into the aqueous phase as a complex mixture of soluble molecules, and (3) photochemical and
48 biological transformations leading to new chemical products (Herrmann et al., 2015).

49 Field experiments to characterise this multiphase medium were developed in the 1950s but increased in the 1980s
50 because of precipitation acidification through sulphur oxidation in cloud droplets (Munger et al., 1983; Hoffmann,
51 1986; Kagawa et al., 2021). These studies have highlighted that cloud and fog processing is efficient and plays a
52 major role in air pollution by transforming gases and aerosol particles. Numerous investigations have focused on
53 inorganic compounds that control aqueous-phase acidity (Pye et al., 2020). The production of strong acids has
54 been assessed because it increases particle mass when clouds/fogs evaporate and leads to acidic deposition when
55 clouds precipitate (Tilgner et al., 2021). Early in the 1990s and much more so in the 2000s, researchers investigated
56 the composition of dissolved organic matter in cloud/fog water which has multiple natural and anthropogenic
57 sources of primary or secondary origins (Herckes et al., 2013). Based on scientific issues, specific classes of
58 compounds have been targeted, such as short-chain carboxylic acids and carbonyls (Löflund et al., 2002; Munger
59 et al., 1995; Sun et al., 2016) and more recently carbohydrates and amino acids (Triesch et al., 2021; Renard et al.,
60 2022). Attention has also been paid to the detection of pollutants with strong sanitary effects, such as polycyclic
61 aromatic hydrocarbon (PAH), phenols, and phthalates (Lüttke et al., 1999; Li et al., 2010; Lebedev et al., 2018;
62 Ehrenhauser et al., 2012) because they can impact ecosystems through precipitation (Wright et al., 2018). Recent
63 investigations using high-resolution mass spectrometry have revealed the complexity of the organic matrix, with
64 thousands of detected molecules (Zhao et al., 2013; Cook et al., 2017; Bianco et al., 2018; Sun et al., 2021). This
65 organic matter is processed during the cloud lifetime and has raised new scientific questions such as the formation
66 of secondary organic aerosol by aqueous phase reactivity (“aqSOA”) (Blando and Turpin, 2000; Lamkaddam et
67 al., 2021) and light absorbing material referring to brown carbon (“BrC”) (Laskin et al., 2015). Microorganisms
68 are also present and active in cloud droplets (Amato et al., 2005; Vařtilingom et al., 2012; Xu et al., 2017; Hu et
69 al., 2018). They can be incorporated because they serve as cloud condensation nuclei (Bauer et al., 2002;
70 Deguillaume et al., 2008) and can impact cloud water composition through their metabolism by consuming or
71 producing new molecules (Liu et al., 2023; Vařtilingom et al., 2013; Pailler et al., 2023). Many investigations have
72 focused on biological cloud characterisation (Amato et al., 2017; Wei et al., 2017).

73 Monitoring cloud chemical and biological compositions is crucial for evaluating the role of key environmental
74 parameters such as emission sources, atmospheric transport and transformations, and physicochemical cloud
75 properties such as cloud acidity or microphysical cloud properties (liquid water content [LWC] and size
76 distribution of cloud droplets). Specific sites or aircraft campaigns allow the collection of cloud water influenced
77 by marine (Macdonald et al., 2018; Gioda et al., 2011), continental (Van pinxteren et al., 2016; Hutchings et al.,
78 2009; Lawrence et al., 2023; Van Pinxteren et al., 2014) and urban emissions (Li et al., 2020; Guo et al., 2012;
79 Herckes et al., 2002) over various continents (mainly Europe, North America, Asia). Owing to their poor
80 accessibility and remoteness, certain geographical locations have been less investigated, such as the Arctic region
81 (Adachi et al., 2022), tropical environments (Dominutti et al., 2022), or marine surfaces (Van Pinxteren et al.,
82 2020). Field experiments combining cloud water and gaseous phase chemical characterisation have also been

83 conducted to evaluate the partitioning of molecules between these two phases and whether bulk cloud water obeys
84 Henry's law (Van Pinxteren et al., 2005; Wang et al., 2020). Bulk aqueous cloud media are used for laboratory
85 investigations to study the aqueous transformations induced by light and the presence of microorganisms
86 (Schurman et al., 2018; Bianco et al., 2019).

87 Therefore, the scientific community requires regular and long-term measurements of cloud chemical and biological
88 parameters. However, cloud sampling procedures are challenging. In recent decades, different samplers have been
89 developed and deployed in the field, which can be operated under specific environmental conditions and present
90 different collection efficiencies possibly impacted by meteorological conditions. These are commonly based on
91 the impact of cloud droplets on the collector surface and avoid the collection of small droplets (<5 µm in diameter).
92 Their collection efficiency and 50% collection cutoff diameter (d₅₀) were calculated and estimated to evaluate the
93 accuracy of droplet collection by the sampler. Monitoring of the microphysical cloud properties (LWC and size
94 distribution) is required to assess this. These samplers refer to "bulk" cloud water collectors because they group
95 droplets of different sizes. Many types of collectors can be listed: active or passive ground- or aircraft-based, and
96 single- or multi-stage. Passive collectors are dependent on wind speed because the air needs to flow through them,
97 allowing sampling. Active collectors are ground-based collectors through which air-containing droplets are forced
98 to flow inside the system by devices such as pumps or ventilator fans. They have been designed and commonly
99 used to obtain higher volumes of water required for laboratory investigations. Ground-based samplers are easy to
100 install, inexpensive, and suitable for long-term observations. Samplers installed on aircrafts are less widely used,
101 and recent developments by Crosbie et al. presenting a new axial cyclone cloud water collector have shown to
102 strongly improve the collection efficiency of cloud droplets compared to previous samplers (Crosbie et al., 2018).
103 All these samplers are described in reviews where their designs, their advantages, limitations are presented (Roman
104 et al., 2013; Skarżyńska et al., 2006).

105 Two types of ground-based active samplers are often used by the scientific community to monitor cloud chemistry
106 and microbiology: the Cloud Water Sampler (CWS) from Vienna University (Kruisz et al., 1993) and the Caltech
107 Active Strand Cloudwater Collector (CASCC) from California Institute of Technology (Daube et al., 1987; Demoz
108 et al., 1996; Collett Jr et al., 1990). These collectors have been adapted for long-term monitoring (Gioda et al.,
109 2013; Guo et al., 2012; Deguillaume et al., 2014; Renard et al., 2020) and specific field campaigns (Wieprecht et
110 al., 2005; Van pinxteren et al., 2016; Li et al., 2017; Li et al., 2020; Bauer et al., 2002).

111 The Puy de Dôme (PUY) station is a reference site for the collection of cloud water from samples collected between
112 2001 and the present. Historically, the CWS sampler has been widely used for microbial and chemical atmospheric
113 studies at this site (Marinoni et al., 2004; Marinoni et al., 2011; Bianco et al., 2017; Joly et al., 2014). This model
114 can collect wet or supercooled droplets, even at high wind speeds. It is made of aluminium or Teflon; the collection
115 vessel can be removed for sterilisation and cleaning. However, the collected water volume of 10–60 mL per hour
116 is a limit for chemical and microbial analyses that require increasing volumes. For long collection times, the vessel
117 should be removed regularly to transfer the water into a sterile storage bottle. These manipulations expose the
118 samples to contamination. The aspiration system must be powerful and, consequently, heavy and energy-
119 consuming, which limits mobile sampling. The objective of this study was to present a ground-based cloud
120 collector that responds to different constraints. This tool should be suitable for analysing cloud microbiology and
121 chemistry, easy to clean and sterilise, allow the collection of high volumes of water, and be easy to deploy for field

122 campaigns (light and low energy consumption). To achieve these objectives, we developed these last years a
123 collector named BOOGIE. This study describes this instrument and compares it to other commonly used samplers
124 to evaluate its efficiency.

125 **2 Materials and Methods**

126 **2.1 Conception of the BOOGIE cloud collector**

127 The 3D drawing was performed with Autodesk® Inventor 2016 and recently updated using the 2019 version. The
128 prototype of the collector used in this study was fabricated on an aluminium stand (Al 5754 and 6060). This
129 material exhibits robust properties and can be easily sterilised by autoclaving before field collection. Aluminium
130 plates were cut using a laser and folded using a metal press. The collection funnel was adapted to a GL 45 thread
131 to directly screw borosilicate glass or polytetrafluoroethylene (PTFE) bottles. All the aluminium parts were treated
132 by QUANALOD® anodisation, with thickness of 20 µm, suitable for aluminium objects exposed to harsh
133 environmental conditions. All parts were thoroughly cleaned to eliminate all manufacturing residue and several
134 cycles of sterilisation by autoclaving (121°, 20 min per cycle) were performed to clean the collector.

135 The vacuum inside the collector was ensured by an axial fan (EMB-papst®, model 6300TD, S-Force, 40 W, 12 V
136 DC) able to work under wet conditions and temperatures of -20 °C to 70 °C. It has a fan diameter of 172 mm and
137 a theoretical maximum flow capacity of 600 m³ h⁻¹ (manufacturer data). It is equipped with a controlled voltage
138 for speed setting, which allows modulation of the fan velocity according to 10 increasing intensities. To measure
139 the air inlet and outlet velocity, a thermal anemometer efficient from 0.2 to 20 m s⁻¹ was used (model Lutron AM-
140 4204 from RS PRO®).

141 **2.2. Computational Fluid dynamics (CFD) simulations**

142 Finite element modelling and simulations were performed using Simcenter 3D software from Siemens Industry
143 Software Inc., version 2022.1. The solver environment was Simcenter 3D Thermal/Flow Advanced Flow. The
144 flow and particle tracking solvers are proprietary to Maya Heat Transfer Technologies. Other numerical
145 computations and figures were performed using MATLAB version 2021a.

146 The fluid domain is represented by the inner volume of the collector. To compute a realistic flow inside the
147 collector, it is necessary to consider the structure of the collector, which is composed of thin walls and metal plates,
148 to enable air deflection and the collection of cloud water droplets. The Simcenter 3D software allows the generation
149 of a volume or mesh directly from the boundaries of different parts of the collector; however, this method was
150 unsuitable because of the thin inner walls. The fluid domain was built using successive Boolean subtractions by
151 leaving a void in the right place, leading to a realistic geometry of the air volume (**Figure S1a**).

152 A finite element mesh was created using CTETRA4 solid elements. The element size was variable: the internal
153 mesh size was set to 20 mm, whereas the element size was set to 24 mm on the rear faces next to the fan and to
154 only 4 mm on the front face, allowing air deflection and the collection of droplets (**Figure S1b**). The total numbers
155 of elements and nodes were 869 799 and 178 610, respectively.

156 For the air inlet flow, three slots of the collector front face were defined as the inlet flow boundary conditions. The
157 flow direction was perpendicular to the front face and the external absolute pressure was equal to the ambient

158 pressure. For the air outlet flow, air velocity was applied to the rear circular face representing the fan. The
159 magnitude varied according to the velocity ranges. The vector was perpendicular to the face.

160 The fluid is the standard air at the altitude of 1500 m (*i.e.*, summit of the PUY), at 15 °C, with the following
161 physical characteristics: 1.1 kg m⁻³ for the mass density and 1.75 kg m⁻¹ s⁻¹ for the dynamic viscosity.

162 The outlet velocity of the fan can be modulated among 10 intensities. The resulting air inlet volume flows have
163 been measured using a hot-wire anemometer located in front of the slots. The surface area of the fan outlet was
164 17671 mm², and the total area of the three inlet slots was 10900 mm². Therefore, there was a theoretical ratio of
165 1.6 between the air inlet volume flow and the air outlet volume flows. To agree with the measured air inlet volume
166 flow, the outlet velocities for the collector simulations were varied for the CFD simulations between 1 and 10 m
167 s⁻¹ in 1 m s⁻¹ step.

168 Different particles were used in the simulation. The water drops were injected into the flow at the three air-inlet
169 slots. Eight different values of drop diameter were selected between 5 and 20 µm. The water droplets were
170 considered spherical. The drag coefficient was automatically calculated using the Reynolds number. The density
171 of water was assumed to be 1 kg/dm³. Gravity was applied to the cloud particles, and the gravity vector was defined
172 as the $-Z$ axis with an acceleration amplitude of 9.81 m s⁻². The sizes and masses of each particle class are
173 summarised in **Table S1**.

174 In the air flow inside the collector, three vertical plates participated in droplet collection. If cloud water drops
175 impact them, they should flow to the bottom of the funnel. Therefore, there is a specific surface configuration; if
176 the water drops stick to the collection face, they do not rebound.

177 We selected the fully coupled pressure-velocity solver to solve the mass and momentum equations simultaneously
178 for each time step. The solver iterates the pressure and velocity solutions until convergence is achieved at each
179 time step. Modelling fluid flow turbulence is crucial for accurately simulating airflow. The flow solver uses
180 different turbulence models that add a viscosity term to the Navier–Stokes governing equations. The two-equation
181 model computes the viscosity term using two additional equations that are solved in parallel with the Navier–
182 Stokes equations. Among the two-equation models, the k-omega turbulence model was selected for this study. The
183 steady state time step was fixed to 0.01 s for all the model simulations.

184 For the steady-state simulation, the flow was fully developed, and its properties (velocity, pressure, and turbulence)
185 were used in the particle-tracking equation. During the analysis, the software solved the equation of motion for
186 each particle once per time step. Notably, because the particle tracking simulation is independent of the flow
187 simulation, the particles do not affect the 3D flow. The injection duration in the fluid domain was 60 s, which is a
188 good compromise between the relevant calculation and a reasonable simulation time.

189 **2.3 Experiments: inter-comparison of samplers**

190 **2.3.1 Sampling site**

191 The testing site of the different cloud collectors was the observatory of the PUY summit at 1465 m above sea level.
192 It is part of the Cézeaux-Aulnat-Opme-Puy De Dôme (CO-PDD) instrument platform for atmospheric research
193 (Baray et al., 2020). PUY is recognised as a global station in the Global Atmosphere Watch (GAW) network and
194 is part of the European and national research infrastructures Aerosol Cloud and Trace Gases Research

195 Infrastructure (ACTRIS) and the Integrated Carbon Observing System (ICOS). The PUY is often located in the
196 free troposphere, particularly during cloud events, and the characterised air is representative of synoptic-scale
197 atmospheric composition. Various biological, physical, chemical, and cloud microphysical parameters were
198 monitored on-site. For cloud microphysical properties, we use the ground-based scattering laser spectrophotometer
199 PVM-100 for cloud droplet volume measurements from Gerber Scientific, Inc. (Reston, VA, USA). This
200 instrument measures the laser light scattered in the forward direction by the cloud droplets. It allows to evaluate
201 the particle volume density (or LWC: liquid water content) and the particle surface area density (PSA). The
202 effective radius R_{eff} can be calculated using LWC and PSA; it is an estimate of the average size of the cloud droplet
203 population and does not represent the mean physical radius (Guyot et al., 2015). All cloud microbiology and
204 chemistry data are available in the PUYCLOUD database (<https://www.opgc.fr/data-center/public/data/puycloud>).

205 **2.3.2 Cloud collectors**

206 Two bulk cloud collectors were compared with a newly developed BOOGIE collector. These are active ground-
207 based collectors commonly used in cloud field studies. They have different collection efficiencies, resulting in
208 different volumes of cloud water that can be sampled. Cloud water collectors are generally designed to avoid the
209 particles below 5 microns to avoid sampling the interstitial aerosol around the droplets. This is a compromise to
210 obtain a sufficient volume of water with less contamination from dry and deliquescent particles. Typically, the
211 smallest droplets were not sampled. The 50% collection efficiency cutoff, based on the droplet diameter, is often
212 predicted from the impaction theory and strongly depends on the aerodynamic design of the impactor and the air
213 flow rate (Berner, 1988; Schell et al., 1992). The collection efficiency for in situ conditions will depend on the
214 LWC, and the meteorological conditions could strongly perturb the way the collectors are able to impact cloud
215 droplets.

216 ***Caltech Active Strand Cloud water Collector: CASCC2***

217 A compact version of the original CASCC collector was used and lent by the Institut de Radioprotection et de
218 Sûreté Nucléaire (IRSN). This sampler, named CASCC2, was constructed according to the recommendations of
219 Demoz et al. (1996). It has an estimated cutoff diameter of $3.5 \mu\text{m}$ (droplet diameter collected with 50% collection
220 efficiency). This collector has a metal body, stainless-steel collection strands, and a metal collection trough. The
221 airflow passed through a set of six rows of stainless-steel strings (diameter, 0.5 mm) with a velocity of 8.6 m s^{-1} .
222 The strings were vertically tilted 35° . The collector design has been shown to generate a stable airflow inside of
223 $348 \text{ m}^3 \text{ h}^{-1}$. In Demoz et al. (1996), they proposed a correction to estimate the fraction of air that actually induces
224 the sampling of the droplets; this was calculated to be 86%, resulting in a $299 \text{ m}^3 \text{ h}^{-1}$ air flow. The volume fraction
225 of the ambient droplet distribution collected was evaluated in Demoz et al. (1996), who showed that this fraction
226 is close to one over most of the LWC range (superior to 95% $>0.1 \text{ g m}^{-3}$ of LWC). Therefore, at the end, a resulting
227 sampled airflow at $284 \text{ m}^3 \text{ h}^{-1}$ ($4.73 \text{ m}^3 \text{ min}^{-1}$) could be estimated. Cloud droplets coalesce on the strands and fall
228 into a bottle through a Teflon tube owing to the combination of gravity and aerodynamic drag. A description of
229 the sampler is provided in **Figure S2**.

230 The collector body was stainless steel, the inlet contained the impaction rows, and the sample drainage was
231 removed before each sampling for cleaning and sterilisation. A sterilised amber glass bottle was placed under the
232 sample drainage during collection. The CASCC2 was also not operated with a downward facing inlet allowing to

233 exclude the collection of rain. This cloud collector was not adapted for temperatures $<0\text{ }^{\circ}\text{C}$ because droplets freeze
234 upon impaction on metallic strands. Note that an upgraded version of the CASCC family was specifically designed
235 for supercooled cloud sampling, the Caltech Heated Rod Cloud Collector (CHRCC).

236 ***Cloud Water Sampler: CWS***

237 This collector (**Figure S3**) was developed specifically to collect warm and supercooled clouds, which can either
238 freeze upon impaction or be collected directly in the liquid phase (Kruisz et al., 1993; Brantner et al., 1994). It was
239 designed to sample cloud water for specific studies on the detection for example of fungal spores and bacteria in
240 cloud water (Tenberken-Pötzsch et al., 2000; Bauer et al., 2002). It comprises a single-stage impactor backed by a
241 large wind shield (50 cm wide and 50 cm high) installed in front of the wind. The wind velocities were reduced in
242 front of the shield, and the flow was directed into the single-slit nozzle. Cloud droplets ranging up to $100\text{ }\mu\text{m}$ in
243 diameter were estimated to be stopped in front of the shield, stay airborne, and were sampled from a stagnant flow.
244 Cloud droplets, which were drawn through a slit 25 cm long and 1.5 cm wide, collided on a rectangular aluminium
245 collection plate installed horizontally, and water was collected in a reservoir below the plate. This sampler model
246 presents an estimated cutoff diameter at 50% collection efficiency of $7\text{ }\mu\text{m}$ at a sampling rate of $86\text{ m}^3\text{ h}^{-1}$, as
247 indicated in Brantner et al. (1994). The CWS used at the PUY was a homemade collector following the
248 recommendation formulated by Kruisz et al. (1993); however, the suction system presented its own characteristics,
249 with an inlet air velocity of 13.5 m s^{-1} . As explained below for Boogie collector, inlet velocity measurement with
250 hot-wire anemometer should be taken with care.

251 The blower was placed under the sampler and connected to the collector body via tubing. This was built of
252 aluminium, and the collection plate and vessel were removable for cleaning and sterilisation. In contrast to the
253 CASCC2, in which the water sample flowed into a glass bottle, in the CWS, the water remained in the collection
254 vessel during the sampling period. It is not possible to check the collected volume during sampling, and the water
255 must be regularly removed by opening the collector and transferring it to a storage bottle. This collector has been
256 used for studies at PUY since the 2000s (Marinoni et al., 2004) because the collection plate and vessel can be
257 sterilised in the laboratory, allowing for microbial analysis of cloud waters.

258 **2.3.4 Chemical and microbial analysis**

259 Chemical and biological analyses were performed on the cloud samples following the standardised procedures
260 described in Deguillaume et al. (2014). The main ions (Cl^- , NO_3^- , NH_4^+ , SO_4^{2-} , Na^+ , Ca^+ , Mg^+ , K^+) were analysed
261 using ion chromatography. Formaldehyde and hydrogen peroxide levels were measured using derivatisation
262 methods and analysed by fluorimetry. Total microbial cell counts, including bacterial, yeast, and fungal spores,
263 were determined using flow cytometry. The microbial energetic state was determined by measuring ATP and ADP
264 concentrations using bioluminescence. More information on this analysis is given in the Supplementary
265 Information.

266 **2.3.5 Back-trajectory analysis**

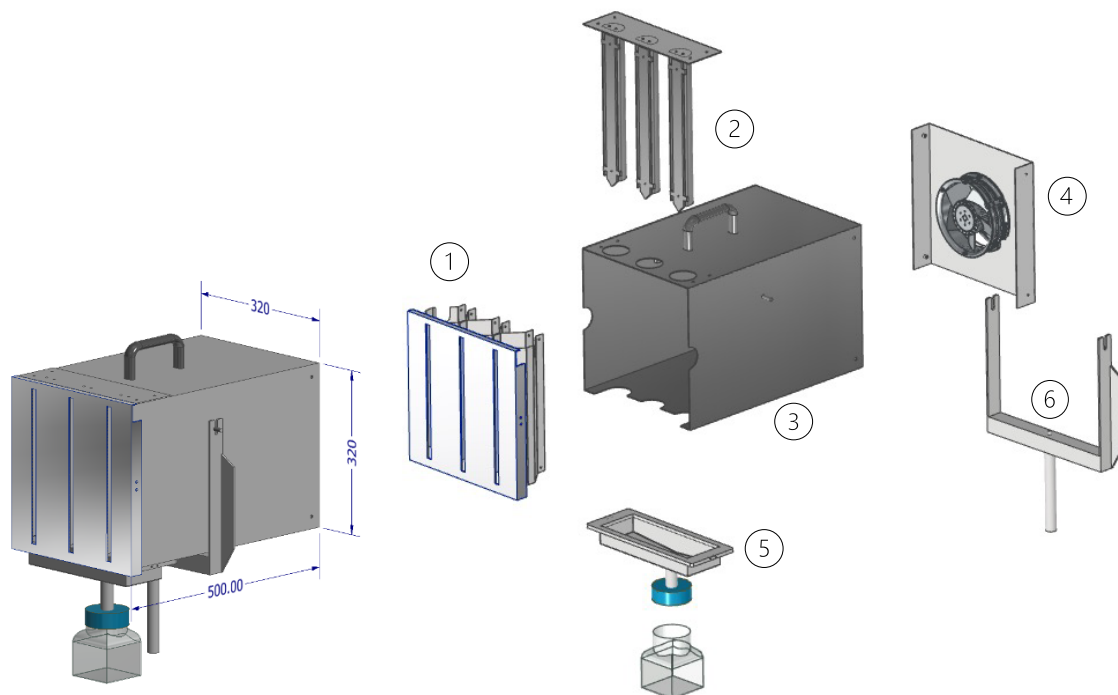
267 The CAT model (Baray et al., 2020) was used to estimate the air mass history reaching the summit of the PUY
268 Mountain during the cloud-sampling period. This model uses the ECMWF ERA-5 wind fields and integrates a

269 topography matrix; back trajectories were calculated every hour during cloud sampling; the temporal resolution
270 was 15 min, and the total duration was 72 h. These calculations are fully described by Renard et al. (2020).

271 3 Results

272 3.1 Conception and operating principles of the BOOGIE collector

273 The new collector is a single-stage collector that uses impaction to sample the cloud droplets (Marple and Willeke,
274 1976). The collector is designed as a slit impactor. **Figure 1** shows the assembled collector (left) and the different
275 parts of the collector and how they should be assembled for sampling. A GIF animation (**Movie 1**) showing the
276 assembly of the collector before sampling is provided in the Supplementary Information. A photograph of the
277 collector is shown in **Figure S4**, and all the dimensions are detailed in **Figure S5**. Parts 1, 2, and 5 were sterilised
278 by autoclaving before sampling to allow for biological analysis.



279
280 **Figure 1. Schematic of the design of the BOOGIE collector. Assembly of the different parts of the BOOGIE collector:**
281 **(1) front face with the three slots; (2) impactation plates; (3) collector body; (4) rear face with the fan; (5) funnel; (6)**
282 **instrument holder.**

283 The cloudy air entered via three rectangular inlets oriented vertically side by side, each 30 cm long and 1.2 cm
284 wide, with 9 cm between them. The droplets were impacted by inertia on aluminium plates located 45 mm behind
285 the air inlets. The inlet width and distance between the inlet and impactation plate were selected to be identical to
286 those of the CWS. The air and smaller non collected droplets were directed to a shared corridor before the air fan.
287 The collected water flowed to the collection funnel under gravity, and the collection bottle was sterilised.

288 3.2 Evaluation of the air flow inside the BOOGIE collector

289 The fan can be modulated at 10 intensities (10–100% of the maximum fan speed). Two ways have been
290 investigated to calculate the air flow through the collector: either by measuring the air inlet velocities at the slots,

291 or by measuring the air outlet velocities. First, the air inlet velocities were measured in front of each of the three
292 slots of the BOOGIE collector at different heights (high, middle, and low points), using a hot-wire anemometer,
293 with the velocity modulated according to these 10 values (**Figure S6**). The measured velocities varied from 2 to
294 approximately 15 m s^{-1} , with an increase of approximately 1.5 m s^{-1} per intensity step. The air inlet velocity
295 stabilized at 90% of the fan speed (corresponding to a measured value of 14 m s^{-1}). By positioning the anemometer
296 identically at each measuring point, the measured velocities at different fan intensities were homogeneous between
297 slots and for the same slot at different heights. However, the positioning of the anemometer is quite sensitive, since
298 a slight displacement can lead to significant measurement deviations. This finding of air velocity heterogeneity at
299 the slots will also be discussed in section 3.3.1.

300 Therefore, we designed an experiment to measure the air flow at the collector outlet. The airflow rate at the fan
301 outlet was measured using the following procedure. A 3.5 m long PVC pipe with an internal diameter of 154 mm
302 was installed after the fan outlet. This diameter enables the entire flow to be measured without reduction, thus
303 limiting the additional pressure losses generated by the addition of the pipe. A hot-wire anemometer was installed
304 in the tube at 3 m from the fan. The large distance/diameter ratio (greater than 19) minimizes disturbances (high
305 turbulence and vortex rates) as the air passes through the axial fan.

306 The flow velocity profile is measured every 5 mm along the diameter. Flow rate is calculated by summing the
307 average velocity for each ring by the ring area. The flow rate was estimated at $433 \text{ m}^3 \text{ h}^{-1}$ at 90% of the fan speed.
308 The average velocity in the pipe is found by dividing the flow rate by the cross-sectional area, which corresponds
309 to a velocity of 6.5 m s^{-1} . Based on this velocity, the Darcy-Weisbach formula and the Moody diagram (with a
310 relative roughness of $2 \cdot 10^{-5}$), the pressure drop in the pipe is estimated at 10 Pa. As a result, the addition of the
311 pipe has little influence on the flow rate.

312 The pressure drop in the BOOGIE impactor can be estimated from the fan and flow characteristics. Since the flow
313 rate has been calculated at $433 \text{ m}^3 \text{ h}^{-1}$, the pressure drop compensated by the fan is estimated at 220 Pa, and
314 consequently the pressure drop in the impactor is around 210 Pa. The variation in density is less than 0.0025 kg
315 m^{-3} , i.e. a variation of less than 0.25%. The flow can be considered incompressible, and conservation of flow-
316 volume can be used. The average velocity at the BOOGIE inlet is estimated at 11 m s^{-1} , by dividing the flow by
317 the inlet cross-section of $10.9 \cdot 10^{-3} \text{ m}^2$. This average velocity differs from the measured velocity at inlet (14 m s^{-1})
318 due to the velocity profile at the slots. The measurement corresponds to a maximum velocity.

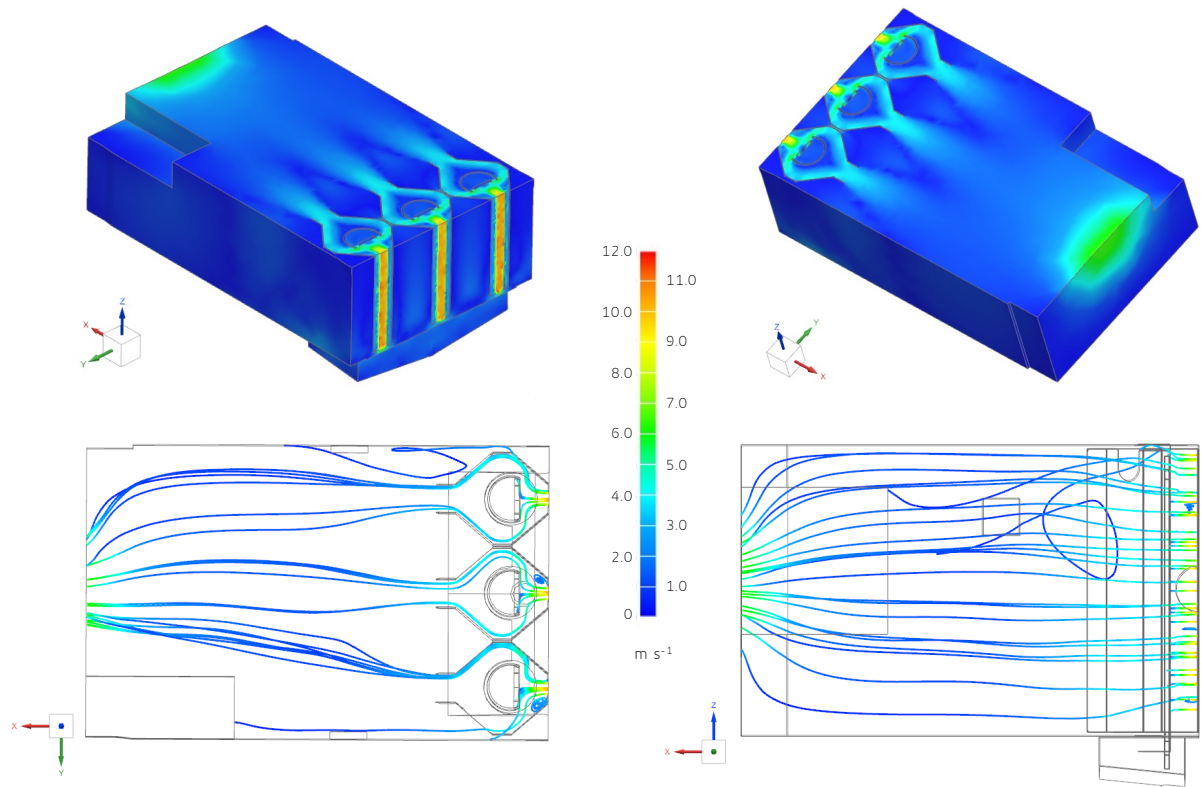
319 **3.3 Performance evaluation**

320 **3.3.1 CFD simulations**

321 *Flow velocity*

322 Several simulations were performed modulating the air outlet velocity from 2 to 10 m s^{-1} . Use of air outlet velocity
323 as boundary condition avoids imposing direction and velocity distribution at inlet. **Figure 2a and b** displays the
324 flow velocity field inside the collector for air outlet flow velocity equal to 6.5 m s^{-1} based on its experimental
325 evaluation presented in section 3.2. (the same for 2 m s^{-1} in **Figure S7a and b**). The air outlet flow velocity equal
326 to 6.5 m s^{-1} corresponds to a mean air inlet flow velocity equal to 11 m s^{-1} (1.6 factor). Experimentally, we measured
327 the air inlet flow velocity at a higher value around 14 m s^{-1} . We present the horizontal cutting planes at the centre
328 of the fan. Regardless of the air outlet velocity, the colour display of the flow velocity contour is identical. We can

329 notice that the velocity simulated close to the slots are heterogeneous confirming the difficulty of robustly
330 measuring input speed.

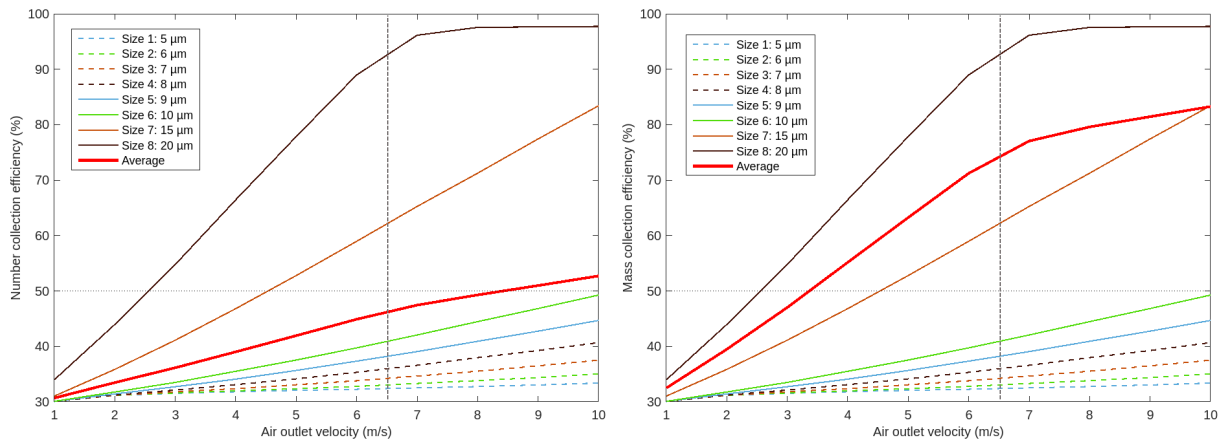


331
332 **Figure 2. a) and b) Cutting plane in the flow velocity contour (in magnitude) in the case of an 6.5 m s^{-1} air outlet flow**
333 **velocity; c) and d) set of streamlines in the collector (c- right view, d - top view) in the case of an 6.5 m s^{-1} air outlet flow**
334 **velocity. Colour code indicates the different air velocity inside the collector.**

335 Streamlines were also displayed (**Figures 2c and d and S7c and d**), with a set of seed points selected randomly
336 on the air inlet faces. They displayed velocity results by showing the path taken by a massless particle. Each point
337 along a streamline is always tangential to the velocity vector of the fluid flow. Again, the streamlines were only
338 slightly modified between the two velocities.

339 ***Particle impact tracking***

340 Various radius sizes of particles were injected into the collector at different air outlet velocities. **Table S2** lists the
341 number of water droplets for each air outlet velocity and each size of particles (from 5 to $20 \mu\text{m}$ in diameter)
342 recorded by the solver in front of the three inlets, represented by the three slots. Arbitrarily, approximately $60\,000$
343 particles are injected. We calculated the number of injected droplets that impacted the vertical plates among the
344 $60\,000$ particles; this allowed to calculate the normalized efficiency of particle collection for each size of particle
345 and each velocity. **Figure 3** reports the efficiency of collection in terms of the number of droplets and the mass of
346 the droplets.



347

348
349

Figure 3. Normalized efficiency of the particle collection, regarding the number of droplets (a) and regarding the mass of the droplets (b) for different diameter size of particle.

350

We can observe that as the air outlet velocity increases, so does the collection efficiency for all droplet sizes. For sizes 7 and 8 (more than 15 μm in term of diameter), the number collection efficiencies were >50% for velocities superior to 4.5 m s⁻¹. At higher speeds, number collection efficiencies >80% were achieved for both size classes. At the maximum speed, a collection efficiency of approximately 50% was reached for size 6 (10 μm in diameter). Considering the mass of the droplets, the two largest sizes (15 and 20 μm in diameter) naturally represented the largest mass of water collected. Because these two sizes were efficiently collected even at low air velocities, a collection efficiency of 50% in terms of mass was achieved at 3 m s⁻¹ of velocity. At 6.5 m s⁻¹ velocity, the average collection efficiency was approximately 75% and 47% in terms of mass and number, respectively.

358

At 6 m s⁻¹, we observed a slowdown in the overall collection efficiency because the largest drops were already 100% collected. These results allowed us to estimate the theoretical cutoff diameter at approximately 12 μm when the air outlet velocity is 6.5 m s⁻¹.

360

361

These results are subject to limitations and uncertainties related to the modelled physical phenomena. First, the statistical results from the CFD simulations were based on a certain number of particles injected into the computational domain to achieve reasonable computing times. Second, the collection surfaces are supposed to be “ideal”: a droplet, that impacts a plate, sticks to it; therefore, its transport by gravity to the funnel remains hypothetical. Third, none of the physical phenomena were considered; the simulations were based on the equations of classical fluid mechanics, but other phenomena, such as electrostatics or Brownian motion, may affect the lightest particles. And last, we can also mention that the air outlet velocity estimated experimentally is also subject to uncertainties that could impact the evaluation of the cutoff diameter. However, the performed simulations indicate that the new BOOGIE collector is able to collect cloud droplets, which also confirms that the distance between the air inlet slots, and the outlet fan is adequate because it is beneficial for air flow stabilisation.

371

3.3.2 Field sampling experiments

372

To evaluate the performance of the BOOGIE sampler, 21 cloud events were collected at PUY station over the period 2016-2024 and the collected water mass as a function of the sampled volume of air was measured (Wieprecht et al., 2005; Demoz et al., 1996). In our database, we selected these events based on the availability of LWC measurements and of the measured mass of the collected water. **Table S3** reports various parameters measured during the sampling duration: meteorological parameters (temperature and wind speed) and

376

377 microphysical cloud properties (Liquid Water Content LWC_{meas} , and effective radius, R_{eff} , every 5 min). These
 378 cloud events were in warm conditions between -1 to 11 °C with moderate wind speed (0.2 to 16 m s⁻¹) and a LWC
 379 from 0.11 to 0.71 g m⁻³. In 2021, 3 cloud events were collected using two BOOGIE collectors deployed in parallel
 380 (corresponding to S1 and S2 samples). In 2024, the collection with two collectors was systemically done and
 381 several samples were collected consecutively during 4 cloud events (15/04/2024, 25/04/2024, 26/04/2024 and
 382 29/04/2024). At the end, 39 samples were used to estimate the BOOGIE collector.

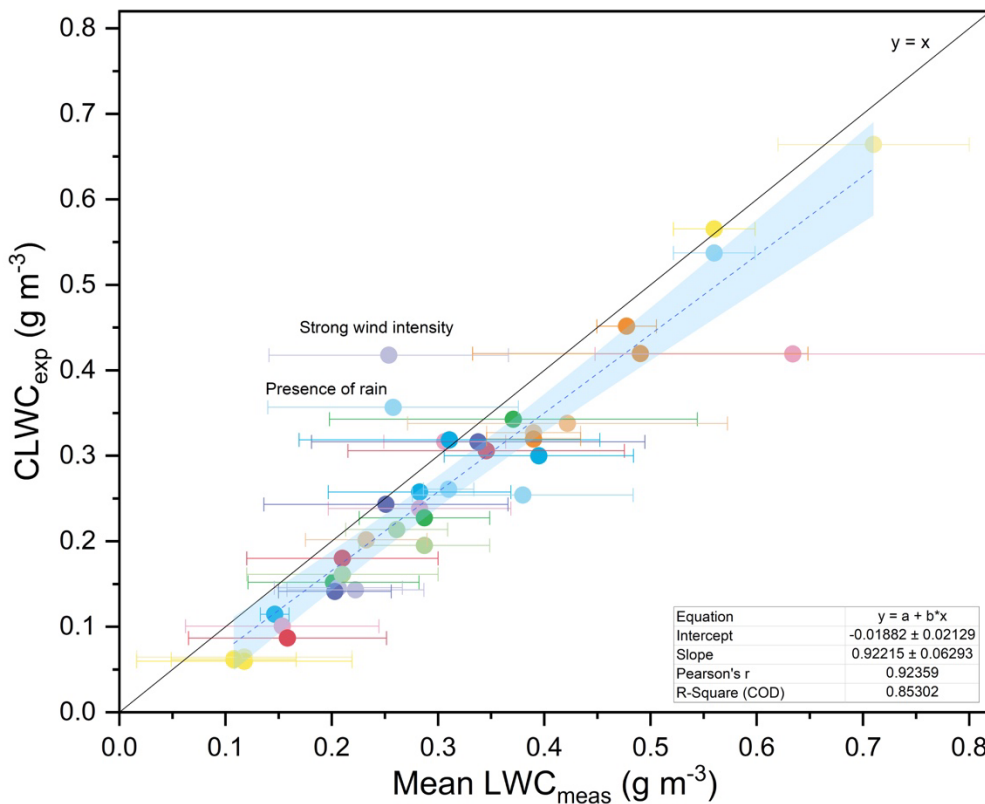
383 First, we can estimate the cloud water collection rates of BOOGIE equal to 100 ± 53 mL h⁻¹. Water volume is
 384 crucial because it determines the biological and chemical analyses that can be performed in the laboratory. The
 385 BOOGIE collection rate allows sufficient cloud water to be obtained in a short duration, which is crucial because
 386 the origin of the air mass that reaches the collection site can vary in a short time.

387 Experimentally, we can also evaluate the Collected LWC ($CLWC_{exp}$) in g m⁻³ (Waldman et al., 1985) as:

$$388 \quad CLWC_{exp} = \frac{M}{F \times \Delta t} \quad (1)$$

389 where M is the collected water mass (g); F is the sampler airflow (m³ min⁻¹); and Δt is the sampling duration (min).

390 To evaluate $CLWC_{exp}$, we estimated in section 3.2, the sampled air flow experimentally at 433 m³ h⁻¹ (7.22 m³
 391 min⁻¹). In this calculation, we were not able to distinguish the fraction of the air that induced the impaction of
 392 droplets as evaluated for the CASCC2 by Demoz et al. (1996). $CLWC_{exp}$ can be compared with the measured mean
 393 LWC_{meas} for the 21 cloud events (i.e., 39 samples), as shown in **Figure 4**.



394
 395 **Figure 4.** Collected cloud water content $CLWC_{exp}$ vs measured LWC_{meas} (in g/m³) for a selection of 21 cloud events
 396 samples at the PUY station. The standard deviation of the measured LWC is indicated. The black solid line represents
 397 the $y = x$ function; linear fit of the experimental data is represented by the dotted blue line and the blue area denotes
 398 the 95% confidence interval of this fit.

399 The $CLWC_{exp}$ and measured LWC_{meas} were well correlated (the slope of the linear regression was 0.92, and the
400 intercept was -0.02 g m^{-3}). Systematic and random deviations from the “theoretical” efficiency are represented by
401 a 1:1 line. Among the 23 cloud samples, only 2 cloud events presented a $CLWC_{exp}$ significantly higher than the
402 LWC_{meas} . Explanations can justify this bias: the cloud event collected the 3/04/2024 present high wind speed with
403 a period during the sampling (20 min) where it reached 16 m s^{-1} and the cloud event sampled the 29/04/2024 was
404 characterized by the presence of a fine rain at the end of the sampling period.

405 The sampling efficiency can be estimated as follows:

$$406 \text{ Sampling efficiency (\%)} = \frac{CLWC_{exp}}{LWC_{meas}} \times 100 \quad (2)$$

407
408 The average calculated sampling efficiency over 21 cloud events was equal to $73.9 \pm 21.4 \%$. Without considering
409 the two cloud events with significant overestimation of $CLWC_{exp}$ vs LWC_{meas} , the sampling efficiency falls to
410 $69.7 \pm 11\%$. The sampling efficiency does not appear to decrease when there was a shift to higher LWC_{meas} . This
411 phenomena has been observed with other samplers such as the CASCC2, possibly explained by interior collector
412 wall losses for large droplets (Wieprecht et al., 2005).

413 The mean cloud wind speed and effective cloud droplet radius varied between the cloud events. **Figure S8** shows
414 the sampling efficiency vs the three meteorological and microphysical parameters. The 21 clouds were sampled
415 under conditions typically encountered at PUY for cloud sampling under warm conditions and for different
416 seasons: minimal temperatures $> -1 \text{ }^\circ\text{C}$ with a maximum value of approximately $11 \text{ }^\circ\text{C}$; wind speed varying from
417 0.2 to 16 m s^{-1} . No tendency was observed between the sampling efficiency and temperature, supporting the fact
418 that the collector can be operated over different seasons. The collector's orientation towards the wind is important,
419 particularly under strong wind conditions. Incorrect orientation (*i.e.*, not in front of the wind) could drastically
420 reduce collection efficiency, whereas orientation towards strong winds could improve collection efficiency. For
421 the collected cloud events, we observed that the collection efficiency slightly increased with wind speed; however,
422 the strength of the association was small. At high wind speeds (gusts) near 10 m s^{-1} , cloud droplet sampling can
423 be non-isokinetic, explaining the possible perturbation of collection efficiency. We can notice that 4 cloud events
424 (corresponding to 6 samples) were collected during high wind condition (more than 11 m s^{-1}). A problem with the
425 orientation of the collector in strong wind condition can lead to significant gaps in collection efficiency. We cannot
426 rule out the possibility that at some point the collector may not face the wind, leading to a reduction in collection
427 efficiency, or that it may face the wind at very high intensities, leading to sampling in non-isokinetic conditions
428 and inducing collection efficiencies more than 100%. This is clearly seen in these 4 events, which show highly
429 heterogeneous collection efficiencies (from 63.5 to 164.7%). The average effective radius varied from 4.6 to 12
430 μm ; there was no correlation between this parameter and the collection efficiency, indicating adequate collection
431 performance of the collector even for smaller droplets.

432 The collection efficiency calculated herein uses the theoretical total cloud water based on integrated measurement
433 methods (LWC). These estimates must be treated with caution because they are marred by several
434 errors/approximations listed here. These can be the result of the limitations of the instruments themselves (the
435 collector and the PVM probe) and the sampling conditions (wind); with the PVM-100 probe, we cannot optimally
436 capture the time evolution of the LWC because data are recorded every 5 min. Finally, the theoretical sampler

437 airflow used to calculate $CLWC_{exp}$ can be additionally perturbed by the wind condition. Nevertheless, this first
438 comparison provides a rough estimate of the collection performance of the BOOGIE collector, which appears to
439 be suitable for contrasting environmental conditions.

440 **3.4 Comparison of cloud samplers**

441 A field campaign was conducted at PUY in 2016 to compare the new collector with other commonly used samplers.
442 The BOOGIE collector has been deployed to sample clouds together with the CWS used at the PUY station since
443 2001 and the CASCC2 (**Figure S9**). From 1st June to 2nd July, four cloud events were simultaneously collected
444 using these three samplers. The meteorological conditions and microphysical cloud properties were monitored
445 during the cloud events (**Figure S10**). Back trajectories were computed using the CAT model for the four cloud
446 events (**Figure S11**). The three samplers were oriented in front of the wind at the beginning of the sampling period;
447 changes in the wind direction were checked during this period, and the orientation of the collectors was modified
448 accordingly.

449 The prevailing winds during the first two cloud events (01 and 04/06/2016) arrived from the north-northwest and
450 north-northeast directions, whereas the other two (28/06/2016 and 02/07/2016) were locally associated with winds
451 coming from the southwest direction. This last event was also characterized by strong wind speeds of up to 14 m
452 s^{-1} at the end of the sampling time. For the four cloud events, the wind directions did not drastically change during
453 the sampling duration except for on the 4th June where some fluctuations were observed; however, these were not
454 significant because the wind speed was extremely low (0.2 m s^{-1}). Regarding the microphysical properties, the first
455 cloud event presented lower mean measured LWC (0.15 g m^{-3}) in comparison to the others (approximately 0.3 g
456 m^{-3}). In contrast, the average radius was highest for the first cloud event ($10.8\text{ vs }4.5\text{--}6.6\text{ }\mu\text{m}$ in radius). The
457 temperature corresponded to warm cloud conditions (between 6 and 10 °C), allowing the collection of liquid
458 droplets.

459 *Sampling efficiency*

460 First, the cloud water samplers were compared in terms of sampling efficiency, considering the calculated
461 $CLWC_{exp}$ and measured LWC_{meas} (equation (2)). For the CASCC2, the airflow was evaluated following Demoz
462 et al. (1996) (Section 2.3.2). In the calculation presented below, we decided to use the value $348\text{ m}^3\text{ h}^{-1}$ without
463 distinguishing the fraction of “sampled air” from the total air entering the collection system. We motivate this by
464 the fact that with the two other collectors we are not able to estimate this fraction. This will allow to compare
465 collection efficiencies estimated on the same calculation basis. The sampled airflow was evaluated for the CWS,
466 which is a homemade collector that follows the recommendations of Kruisz et al. (1993). As indicated in Section
467 2.3.2, the air inlet flow velocity was measured with a hot-wire anemometer as 13.5 m s^{-1} . Therefore, considering
468 the surface of the entry slot, the sampled air entering the CWS collector was calculated to be equal to $182\text{ m}^3\text{ h}^{-1}$
469 ($3.04\text{ m}^3\text{ min}^{-1}$). We are aware that this estimation is rough since, as for the BOOGIE collector, the measurement
470 of the air flow velocity at the slot entry is difficult since the positioning of the probe induces biases in the
471 measurement.

472

473

474
475

Table 1. Information on cloud water collection performed with BOOGIE, CWS and CASCC2 samplers for four independent cloud events at PUY. The temperature, wind speed and R_{eff} are averaged over the sampling time.

Cloud events: duration, mean temperature, mean wind speed & mean effective radius	Sampler	BOOGIE	CWS	CASCC2
	Airflow ($\text{m}^3 \text{h}^{-1} / \text{m}^3 \text{min}^{-1}$)	433/7.22	182.2/3.04	348/5.8
Date = 01/06/2016	LWC _{meas} (g m^{-3})		0.15 ± 0.01	
Duration = 90 min	Sampled volume of air	650	273	522
T = 6.3 ± 0.2 °C	Collected water (g)	59	19	40
Wind speed = 8.1 ± 0.5 m s^{-1}	CLWC _{exp} (g m^{-3})*	0.09	0.07	0.08
$R_{\text{eff}} = 10.8 \pm 0.7$ μm	Sampling efficiency (%)*	62	47	54
Date = 04/06/2016**	LWC _{meas} (g m^{-3})		0.31 ± 0.06	
Duration = 180 min	Sampled volume of air	1299	545	1044
T = 7.8 ± 0.2 °C	Collected water (g)	326	110	261
Wind speed = 0.3 ± 0.1 m s^{-1}	CLWC _{exp} (g m^{-3})*	0.251	0.202	0.250
$R_{\text{eff}} = 6.6 \pm 0.6$ μm	Sampling efficiency (%)*	84	66	82
Date = 28/06/2016	LWC _{meas} (g m^{-3})		0.35 ± 0.13	
Duration = 60 min	Sampled volume of air	433	182	348
T = 9.3 ± 0.14 °C	Collected water (g)	105	34	88
Wind speed = 2.3 ± 0.4 m s^{-1}	CLWC _{exp} (g m^{-3})*	0.243	0.187	0.253
$R_{\text{eff}} = 4.6 \pm 1.0$ μm	Sampling efficiency (%)*	71	54	73
Date = 02/07/2016	LWC _{meas} (g m^{-3})		0.26 ± 0.05	
Duration = 360 min	Sampled volume of air	2599	1091	2088
T = 9.7 ± 1 °C	Collected water (g)	440	135	290
Wind speed = 12.0 ± 1.5 m s^{-1}	CLWC _{exp} (g m^{-3})*	0.169	0.124	0.139
$R_{\text{eff}} = 6.1 \pm 0.7$ μm	Sampling efficiency (%)*	65	48	54

* The collected LWC (CLWC_{exp}) is calculated following equation (1) and the sampling efficiency by equation (2); ** Fine raining event before the end of sampling.

476

477 The CASCC2 and BOOGIE samplers collected between 348 to 433 m^3 of air per hour, whereas the sampled
478 volume of air collected by the CWS was markedly lower (around 180 $\text{m}^3 \text{h}^{-1}$), which explains the lower amount of
479 collected water. The BOOGIE sampler presented a mean water collection rate for the four cloud events of 82 ± 32
480 mL h^{-1} . This was significantly higher than the rates obtained with the other collectors (CASCC2: 62 ± 30 mL h^{-1} ;
481 CWS : 26 ± 11 mL h^{-1}) (t-test, $p < 0.05$). On average, the calculated sampling efficiencies were $70 \pm 10\%$, $53 \pm 9\%$,
482 and $66 \pm 14\%$ for BOOGIE, CWS, and CASCC2, respectively. Overall, the three collectors exhibited similar and
483 satisfactory collection efficiencies.

484 Wieprecht et al. (2005) highlighted that the CASSC2 collection efficiency could be impacted by the loss of droplets
485 off the strands and/or losses inside the collector on the walls, as highlighted by particularly for large droplets. This
486 collector appeared to be more affected by the intensity of wind speed, with the lowest collection efficiencies
487 observed for the two windier cloud events. As reported by Krusz et al. (1992) for CWS and shown in this study
488 for BOOGIE, no correlation of wind speeds to the CLWC_{exp} of the samplers was found. In the case of the 4th June
489 cloud, the appearance of fine rain during sampling could possibly explain the higher collection efficiency observed
490 for all collectors, as we did not observe conditions such as strong winds that could disrupt the sampling.

491 Concerning the CASCC2, a sampling efficiency was previously determined during the FEBUKO experiments in
 492 the Thüringer Wald (Germany) at $56 \pm 17\%$ (Wieprecht et al., 2005). This sampling efficiency for the CASCC2
 493 seems to be slightly lower than that calculated in the present study. Kruiz et al. (1993) calculated a sampling
 494 efficiency of approximately 60% for the CWS during sampling experiments performed at Mount Sonnblick
 495 (Austria) in the same range of order than in the present study. The sampling efficiency depends on environmental
 496 conditions and cloud microphysical properties, which differ between collection sites, explaining this variability.
 497 The four cloud events have also been sampled at PUY under “optimal” conditions (summertime conditions with
 498 limited wind speed and sufficient cloud LWC), possibly explaining the efficient collection of the samplers.

499 *Cloud water chemical and biological composition*

500 To compare the three cloud water collectors, we also focused on the chemical compositions of the three cloud
 501 water samples collected in 2016. The concentrations of inorganic ions in samples collected with the CWS and
 502 CASCC2 collectors (**Table S4, Figure S12**) were compared to the concentrations measured in samples collected
 503 with BOOGIE using the discrepancy factor (D_f) calculated using **equations 3a and 3b**.

$$504 \quad D_{f,CWS} = \frac{C_{BOOGIE} - C_{CWS}}{\left(\frac{C_{BOOGIE} + C_{CWS}}{2}\right)} \quad (3a)$$

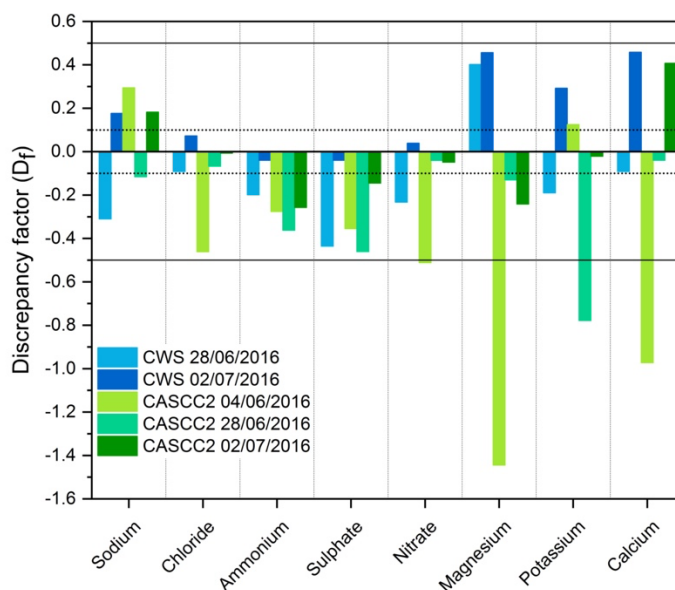
$$505 \quad D_{f,CASCC2} = \frac{C_{BOOGIE} - C_{CASCC2}}{\left(\frac{C_{BOOGIE} + C_{CASCC2}}{2}\right)} \quad (3b)$$

506 where C_{BOOGIE} is the concentration of ions measured in samples collected with BOOGIE, and C_{CWS} and C_{CASCC2}
 507 are the concentrations of ions measured with CWS and CASCC2, respectively.

508 **Figure 5** shows the estimated $D_{f,CWS}$ and $D_{f,CASCC2}$ for anions and cations for cloud samples. The horizontal dashed
 509 lines represent the analytical error on the measurement, which is comparable with $D_{f,CWS}$ 02/07/2016 for sulphate,
 510 nitrate, chloride, and ammonium and $D_{f,CASCC2}$ 28/06/2016 and 02/07/2016 for nitrate, sulphate, chloride, and
 511 sodium. The other D_f values were higher, but generally <0.5 , which could represent a good comparability of the
 512 cloud collectors, because the chemical composition of cloud condensation nuclei may be inhomogeneous. A high
 513 variability by a factor 3 to 6 was observed for the magnesium and potassium ions, but they also present a lower
 514 concentration under 15 and 8 μM , respectively (**Figure S12**). For the most concentrate ions as ammonium (over
 515 150 μM) and nitrate (over 50 μM), their concentrations are comparable between the samplers.

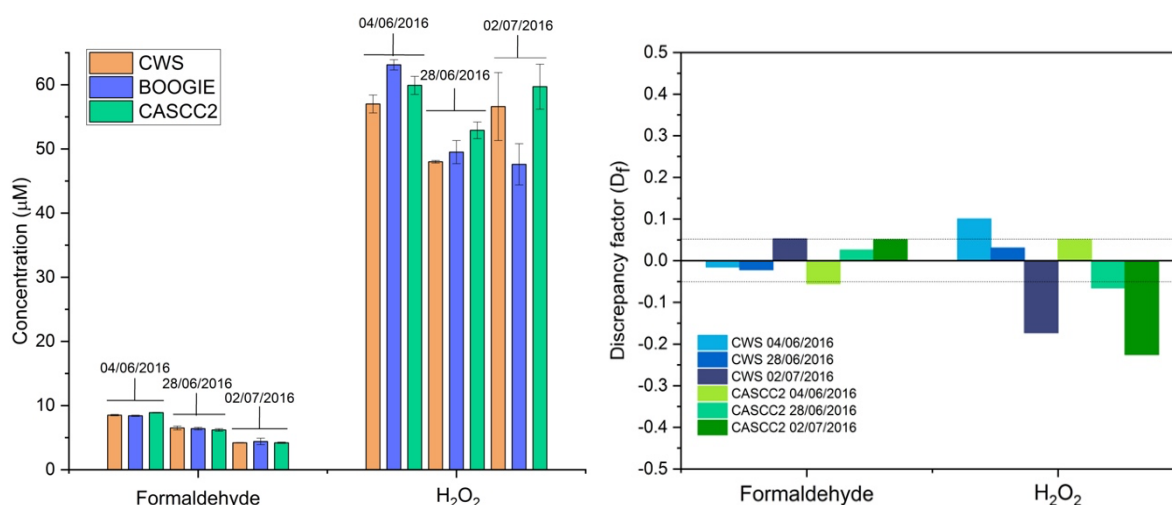
516 At first glance, concentrations with the CASCC2 appear to be slightly higher, but not for all ionic species and not
 517 for all the cloud events. These three samplers present specific designs and surfaces of collection (plate for BOOGIE
 518 and CWS vs strands for CASCC2), leading to different estimated cutoff diameters (12 μm for BOOGIE, 7.5 μm
 519 for CWS, and 3.5 μm for CASCC2) and possibly to differences in the chemical composition of the samples.

520



521
 522 **Figure 5. Histograms presenting discrepancy factors (D_f) between BOOGIE and CWS and CASCC2 calculated using**
 523 **anion and cation concentrations for the three cloud samples. The dashed lines represent the analytical error, whereas**
 524 **the plain line represents the 50% discrepancy.**

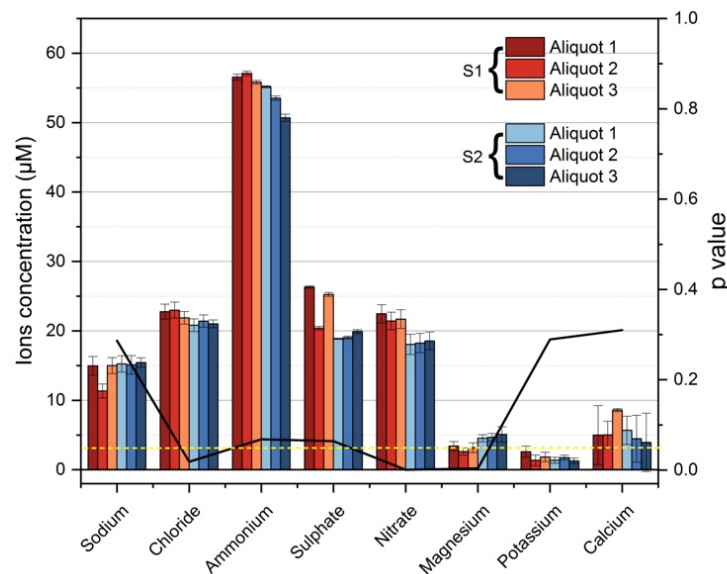
525 Formaldehyde and hydrogen peroxide concentrations have been also measured in samples obtained with the three
 526 collectors. Concentrations and discrepancy factors between collectors are presented in **Figure 6**. These results are
 527 consistent with what was observed with the ionic content because the collectors indicate D_f values mostly within
 528 the analytical error and maximum measured D_f values <0.5 .



529 **Figure 6. Left: Histograms presenting the formaldehyde and hydrogen peroxide concentrations for the three cloud**
 530 **samples collected using CWS, BOOGIE, and CASCC2 in parallel. The error bars correspond to the standard deviation.**
 531 **Right: Histograms presenting discrepancy factors (D_f) between the BOOGIE and CWS and CASCC2. The dashed lines**
 532 **represent the analytical error.**

533 To further evaluate BOOGIE, two identical collectors were installed at the PUY station in 2021 to check for
 534 differences in the chemical composition of cloud waters collected in parallel. For clouds on 08/07/2021, chemical
 535 measurements were performed in triplicate to analyze the statistical differences (**Figure 7, Table S5**). The error
 536 bars depict the analysis error, which is higher than the discrepancy between the BOOGIE collectors for sodium,
 537 potassium, calcium, and chloride. The black plain line represents the p-value obtained for the t-test (right y-axis);
 538 if the p-value is <0.05 , represented in the plot by the yellow dashed line, the difference between the two BOOGIE

539 collectors is significant, as observed for magnesium, nitrate, and chloride. Nevertheless, the difference was not
 540 significant for sodium, ammonium, potassium, calcium, and sulphate, indicating good reproducibility of sampling
 541 with the BOOGIE collectors.



542 **Figure 7. Histograms presenting the concentrations for a specific cloud sampled on 08/07/2021 at PUY with two**
 543 **BOOGIE collectors. This time, three aliquots were analysed twice (error bars) using ion chromatography. p-values are**
 544 **indicated with the black line and the yellow dashed line indicates the threshold of $p = 0.05$.**

545 Given the uncertainties in laboratory measurements and the possible intrinsic variability of the chemical
 546 composition within the cloud system, we can reasonably argue that the chemical compositions of the collectors
 547 are comparable. [Schell et al. \(1992\)](#) compared two single-stage cloud impactors with different designs and
 548 highlighted the large differences between the ionic compositions of the samples. These differences have been
 549 discussed to be related to different microphysical properties of the sampled clouds that induced bias in the
 550 collection: smaller droplets can be sampled with a lower cutoff diameter of the collector, and a lower LWC can
 551 eventually induce some evaporation of the smaller droplets. The three cloud events presented “stable”
 552 microphysical properties during their collection period (**Figure S9**). This could explain the good agreement
 553 between the collectors in terms of their chemical composition. [Wieprecht et al. \(2005\)](#) compared the chemical
 554 composition of cloud water collected with a low-volume single-stage slit jet impactor and with the CASCC2 string
 555 collector and reported 8–15% differences in the solute ionic mass in cloud water, in the range observed in the
 556 present study (4–35% of differences, average of 12%) between the three collectors.

557 The microbial energetic state given by the in-cell ATP and ADP concentrations from each cloud sample was
 558 assessed during the inter-comparison campaign (see Supplementary Information for a description of the protocol).
 559 The ATP/ADP ratio gives the energetic stress of the cloud water microbiota; a ratio <0.6 indicates a good energetic
 560 state, 0.6 to 1, a medium one, and >1 , a low energetic state. The measured ratios are listed in **Table S6**. The
 561 ATP/ADP ratio ranged from 0.2 to 0.4, revealing a good energetic state of microflora for each sample. The
 562 measured ATP/ADP ratios were similar for the cloud water samples from the three collectors. Thus, we argue that
 563 the three samplers could be considered non-stressful and suitable for cloud microbiota collection.

564

565 4 Conclusions

566 This study presented a new cloud collector called BOOGIE. This single-stage collector allows cloudy air
567 containing aqueous droplets to be drawn through three air inlets in the form of vertically oriented slots. The cloud
568 droplets were collected using vertical plates placed behind the slots, allowing them to be impacted. They then
569 flowed by gravity along the plates, fell into a funnel, and ended up in a sterilised glass bottle. It was made of
570 aluminium, but can be manufactured from other materials, such as plastic materials such as nylon or PTFE to
571 investigate transition metal ions in cloud waters. The cloud collector can be connected to the mains or run on
572 batteries (12 V voltage); thus, the collector can be operated at its own power during field measurement campaigns
573 for at least 4 h using a 2 kg small battery. Parts of the sampler were removed for cleaning; the front face, impaction
574 chamber, funnel, and glass bottle were sterilised in an autoclave. This allowed for the characterisation of the
575 biological content of the sampled clouds (biodiversity, concentration, and viability/activity) (Vařtilingom et al.,
576 2012). Biological and chemical collector blanks were easily prepared by spraying MilliQ water onto the collection
577 plates and collecting the water flowing into the collection glass bottle.

578 CFD simulations were performed to investigate how the collector captured cloud droplets. First, considering the
579 3D-dimensional structure of the collector, some turbulences were simulated inside the collector, which was
580 reassuring. Different sizes of cloud droplets were injected into the collector to simulate their impacts on the
581 collection plates. This theoretical study indicates that on average, for all droplet sizes (radius from 2.5 to 10 μm),
582 the average collection efficiencies of $>50\%$ in terms of numbers were achieved at air outlet velocities $>8 \text{ m s}^{-1}$. A
583 collection efficiency of approximately 50% was reached for 5 μm droplets in radius that gave us an estimate of the
584 50% cutoff diameter of the collector (approximately 12 μm). This estimate seems higher than the cutoff diameters
585 of other cloud samplers (more in the range between 3.5 and 10 μm in diameter). However, comparisons of cutoff
586 diameters between samplers are difficult because these estimates are made using different methods; in particular,
587 the theoretical collection efficiency often considers the Stokes number (Demos et al., 1996).

588 Based on the 21 cloud events sampled at the PUY station, a mean water collection efficiency was calculated as
589 $100 \pm 53 \text{ mL h}^{-1}$ for clouds presenting various microphysical cloud properties: the mean LWC was between 0.11
590 and 0.71 g m^{-3} and the mean effective radius R_{eff} was between 4.6 and 11.8 μm . This made it possible to obtain
591 sufficient water volumes over short periods for targeted chemical and biological analyses. This is crucial for
592 minimally integrating the cloud properties in space and time. Methodological developments in recent years have
593 made it possible to assess the organic composition and biodiversity of this aqueous environment using non-targeted
594 methods (Rossi et al., 2023; Bianco et al., 2018). This requires large volumes of cloud water (hundreds of milliliters
595 or even liters of water), which can be collected rapidly using the new collector alone or by duplicating it.

596 Considering the measured LWC, LWC_{meas} , the sampling efficiency of this new collector was estimated at $69.7 \pm$
597 11% over the same set of cloud events collected at PUY. No significant tendency in the collection efficiency was
598 observed as the wind speed increased, over the range of variation between 0.3 to more than 15 m s^{-1} and definite
599 variability in the collection efficiency was observed at high wind condition. No significant correlation was
600 observed between the efficiency and mean measured effective radius. A low LWC cloud event would likely present
601 a greater proportion of liquid water residing in smaller droplets; therefore, for a low LWC, we expected the
602 collection efficiency to diminish owing to the cutoff diameter. However, this decrease was not observed in the

603 cloud samples. Additional measurements of droplet size distribution during sampling would be beneficial for
604 clarifying this issue.

605 We compared the collection efficiency and chemical compositions of the BOOGIE collector with two collectors
606 that are commonly used by the scientific community to study cloud composition and environmental variability:
607 the CWS and the CASCC2. For the four studied cloud events, the BOOGIE collector presented an elevated water
608 collection rate of $82 \pm 32 \text{ mL h}^{-1}$ (CASCC2: $62 \pm 30 \text{ mL h}^{-1}$; CWS: $26 \pm 11 \text{ mL h}^{-1}$). This can be explained by the
609 increased volume of cloudy air entering the new collector. On average, the calculated sampling efficiency was 70
610 $\pm 10\%$ for BOOGIE, in the same range as that for CASCC2 and CWS. The chemical and biological compositions
611 measured in the samples collected by the three collectors can be evaluated as comparable; however, some
612 differences can be highlighted, which can be explained by the design of the collector, type of collection, and
613 inhomogeneous chemical composition of the cloud condensation nuclei.

614 This BOOGIE collector is designed for use in field campaigns and long-term observatory sites. It contributes to
615 the evaluation of the complex cloud water bio-physico-chemical composition, to the analysis of its environmental
616 variability; it allows a sufficient volume of water to be collected to characterize the chemical and biological
617 transformations occurring in it. This will help better constrain detailed cloud chemistry models that need to be
618 validated (Barth et al., 2021). For future development, our team aims to reduce the size and weight of the collector
619 such that it can be installed under a native balloon. The second development concerns the automation of this
620 collector to initiate collection remotely and increase the sampling frequency. Finally, we aim to conduct intensive
621 campaigns in the frame of the ACTRIS “Cloud In Situ” network to compare the collectors used by the scientific
622 community at other measurement sites.

623 *Data availability:* All data are available through communication with the authors.

624 *Author contributions:* LD, MV were responsible of the project. MV, CBern and LD designed the new instrument,
625 MR created the 3D plans of BOOGIE. CBert performed the CFD analysis. MV, AB and LD conducted the cloud
626 sampling. MV and AB performed the chemical and biological analysis in the lab. CG, CV and LD performed the
627 physical measurements to estimate the air flow inside the collector. LD and MV performed the data analysis. LD,
628 MV and AB conducted scientific analyses. LD prepared the manuscript and designed the figures, with
629 contributions from all authors.

630 *Competing interests.* The authors declare that they have no conflict of interest.

631 *Acknowledgments.* This study on cloud water characterisation was performed in the framework of the CO-PDD
632 instrumented site of the OPGC observatory and LAMP laboratory. This study was supported by the Université
633 Clermont Auvergne, Centre National de la Recherche Scientifique (CNRS), and Centre National d’Etudes
634 Spatiales (CNES). The authors are also grateful for the support from the Fédération des Recherches en
635 Environnement through the CPER funded by Region Auvergne–Rhône-Alpes, the French Ministry, ACTRIS
636 Research Infrastructure, and FEDER European regional funds. The authors also thank I-Site CAP 20-25. We thank

637 Olivier Masson from the IRSN for their CASCC2 collector, which was gratefully lent during the inter-comparison
638 campaign.

639 *Financial support.* The authors are grateful to the Agence Nationale de la Recherche (ANR) for its financial
640 support through the BIOCAP (ANR-13-BS06-0004) and METACLOUD (ANR-19-CE01-0004) projects. The first
641 project has financed the work of Mickaël Vaïtilingom during his post-doc at the LAMP laboratory and the second
642 one allowed for their evaluation for specific scientific questions. We thank OPGC for additional funding and
643 OPGC Service de developpement technologique for manufacturing the cloud samplers. The Institut de Chimie de
644 Clermont-Ferrand and Laboratoire Microorganismes: Génome Environnement laboratories are acknowledged for
645 allowing access to their chemical and microbial analytical platforms.

646 **References**

647 Adachi, K., Tobo, Y., Koike, M., Freitas, G., Zieger, P., and Krejci, R.: Composition and mixing state of Arctic
648 aerosol and cloud residual particles from long-term single-particle observations at Zeppelin Observatory, Svalbard,
649 *Atmos. Chem. Phys.*, 22, 14421-14439, 10.5194/acp-22-14421-2022, 2022.

650 Amato, P., Ménager, M., Sancelme, M., Laj, P., Mailhot, G., and Delort, A.-M.: Microbial population in cloud
651 water at the puy de Dôme: Implications for the chemistry of clouds, *Atmos. Environ.*, 39, 4143-4153,
652 <https://doi.org/10.1016/j.atmosenv.2005.04.002>, 2005.

653 Amato, P., Joly, M., Besaury, L., Oudart, A., Taib, N., Moné, A. I., Deguillaume, L., Delort, A.-M., and Debroas,
654 D.: Active microorganisms thrive among extremely diverse communities in cloud water, *PLOS ONE*, 12,
655 e0182869, 10.1371/journal.pone.0182869, 2017.

656 Baray, J. L., Deguillaume, L., Colomb, A., Sellegri, K., Freney, E., Rose, C., Van Baelen, J., Pichon, J. M., Picard,
657 D., Fréville, P., Bouvier, L., Ribeiro, M., Amato, P., Banson, S., Bianco, A., Borbon, A., Bourcier, L., Bras, Y.,
658 Brigante, M., Cacault, P., Chauvigné, A., Charbouillot, T., Chaumerliac, N., Delort, A. M., Delmotte, M., Dupuy,
659 R., Farah, A., Febvre, G., Flossmann, A., Gourgbeire, C., Hervier, C., Hervo, M., Huret, N., Joly, M., Kazan, V.,
660 Lopez, M., Mailhot, G., Marinoni, A., Masson, O., Montoux, N., Parazols, M., Peyrin, F., Pointin, Y., Ramonet,
661 M., Rocco, M., Sancelme, M., Sauvage, S., Schmidt, M., Tison, E., Vaïtilingom, M., Villani, P., Wang, M., Yver-
662 Kwok, C., and Laj, P.: Cézeaux-Aulnat-Opme-Puy De Dôme: a multi-site for the long-term survey of the
663 tropospheric composition and climate change, *Atmos. Meas. Tech.*, 13, 3413-3445, 10.5194/amt-13-3413-2020,
664 2020.

665 Barth, M. C., Ervens, B., Herrmann, H., Tilgner, A., McNeill, V. F., Tsui, W. G., Deguillaume, L., Chaumerliac,
666 N., Carlton, A., and Lance, S. M.: Box model intercomparison of cloud chemistry, *J. Geophys. Res.: Atmos.*, 126,
667 e2021JD035486, <https://doi.org/10.1029/2021JD035486>, 2021.

668 Bauer, H., Kasper-Giebl, A., Löflund, M., Giebl, H., Hitzemberger, R., Zibuschka, F., and Puxbaum, H.: The
669 contribution of bacteria and fungal spores to the organic carbon content of cloud water, precipitation and aerosols,
670 *Atmos. Res.*, 64, 109-119, [https://doi.org/10.1016/S0169-8095\(02\)00084-4](https://doi.org/10.1016/S0169-8095(02)00084-4), 2002.

671 Berner, A.: The collection of fog droplets by a jet impaction stage, *STOTEN*, 73, 217-228,
672 [https://doi.org/10.1016/0048-9697\(88\)90430-5](https://doi.org/10.1016/0048-9697(88)90430-5), 1988.

673 Bianco, A., Deguillaume, L., Chaumerliac, N., Vaïtilingom, M., Wang, M., Delort, A.-M., and Bridoux, M. C.:
674 Effect of endogenous microbiota on the molecular composition of cloud water: a study by Fourier-transform ion
675 cyclotron resonance mass spectrometry (FT-ICR MS), *Sci. Rep.*, 9, 7663, 10.1038/s41598-019-44149-8, 2019.

676 Bianco, A., Deguillaume, L., Vaïtilingom, M., Nicol, E., Baray, J.-L., Chaumerliac, N., and Bridoux, M.:
677 Molecular characterization of cloud water samples collected at the puy de Dôme (France) by Fourier Transform
678 Ion Cyclotron Resonance Mass Spectrometry, *Environ. Sci. & Technol.*, 52, 10275-10285,
679 10.1021/acs.est.8b01964, 2018.

680 Bianco, A., Vařtilingom, M., Bridoux, M., Chaumerliac, N., Pichon, J.-M., Piro, J.-L., and Deguillaume, L.: Trace
681 metals in cloud water sampled at the Puy de Dôme station, *Atmosphere*, 8, 225,
682 <https://doi.org/10.3390/atmos8110225>, 2017.

683 Blando, J. D. and Turpin, B. J.: Secondary organic aerosol formation in cloud and fog droplets: a literature
684 evaluation of plausibility, *Atmos. Environ.*, 34, 1623-1632, 10.1016/s1352-2310(99)00392-1, 2000.

685 Brantner, B., Fierlinger, H., Puxbaum, H., and Berner, A.: Cloudwater chemistry in the subcooled droplet regime
686 at Mount Sonnblick (3106 M A.S.L., Salzburg, Austria), *Water, Air, and Soil Poll.*, 74, 363-384,
687 10.1007/BF00479800, 1994.

688 Collett Jr, J. L., Daube Jr, B. C., Gunz, D., and Hoffmann, M. R.: Intensive studies of Sierra Nevada cloudwater
689 chemistry and its relationship to precursor aerosol and gas concentrations, *Atmos. Environ.*, 24, 1741-1757,
690 10.1016/0960-1686(90)90507-j, 1990.

691 Cook, R. D., Lin, Y. H., Peng, Z., Boone, E., Chu, R. K., Dukett, J. E., Gunsch, M. J., Zhang, W., Tolic, N., Laskin,
692 A., and Pratt, K. A.: Biogenic, urban, and wildfire influences on the molecular composition of dissolved organic
693 compounds in cloud water, *Atmos. Chem. Phys.*, 17, 15167-15180, 10.5194/acp-17-15167-2017, 2017.

694 Crosbie, E., Brown, M. D., Shook, M., Ziemba, L., Moore, R. H., Shingler, T., Winstead, E., Thornhill, K. L.,
695 Robinson, C., MacDonald, A. B., Dadashazar, H., Sorooshian, A., Beyersdorf, A., Eugene, A., Collett Jr, J., Straub,
696 D., and Anderson, B.: Development and characterization of a high-efficiency, aircraft-based axial cyclone cloud
697 water collector, *Atmos. Meas. Tech.*, 11, 5025-5048, 10.5194/amt-11-5025-2018, 2018.

698 Daube, B., Kimball, K. D., Lamar, P. A., and Weathers, K. C.: Two new ground-level cloud water sampler designs
699 which reduce rain contamination, *Atmos. Environ.*, 21, 893-900, [https://doi.org/10.1016/0004-6981\(87\)90085-0](https://doi.org/10.1016/0004-6981(87)90085-0),
700 1987.

701 Deguillaume, L., Leriche, M., Amato, P., Ariya, P. A., Delort, A. M., Pöschl, U., Chaumerliac, N., Bauer, H.,
702 Flossmann, A. I., and Morris, C. E.: Microbiology and atmospheric processes: chemical interactions of primary
703 biological aerosols, *Biogeosciences*, 5, 1073-1084, 10.5194/bg-5-1073-2008, 2008.

704 Deguillaume, L., Charbouillot, T., Joly, M., Vařtilingom, M., Parazols, M., Marinoni, A., Amato, P., Delort, A.
705 M., Vinatier, V., Flossmann, A., Chaumerliac, N., Pichon, J. M., Houdier, S., Laj, P., Sellegri, K., Colomb, A.,
706 Brigante, M., and Mailhot, G.: Classification of clouds sampled at the puy de Dôme (France) based on 10 yr of
707 monitoring of their physicochemical properties, *Atmos. Chem. Phys.*, 14, 1485-1506, 10.5194/acp-14-1485-2014,
708 2014.

709 Demoz, B. B., Collett, J. L., and Daube, B. C.: On the Caltech active strand cloudwater collectors, *Atmos. Res.*,
710 41, 47-62, [https://doi.org/10.1016/0169-8095\(95\)00044-5](https://doi.org/10.1016/0169-8095(95)00044-5), 1996.

711 Dominutti, P. A., Renard, P., Vařtilingom, M., Bianco, A., Baray, J. L., Borbon, A., Bourianne, T., Burnet, F.,
712 Colomb, A., Delort, A. M., Duflo, V., Houdier, S., Jaffrezo, J. L., Joly, M., Lereboure, M., Metzger, J. M.,
713 Pichon, J. M., Ribeiro, M., Rocco, M., Tulet, P., Vella, A., Leriche, M., and Deguillaume, L.: Insights into tropical
714 cloud chemistry in Réunion (Indian Ocean): results from the BIO-MAÏDO campaign, *Atmos. Chem. Phys.*, 22,
715 505-533, 10.5194/acp-22-505-2022, 2022.

716 Ehrenhauser, F. S., Khadapkar, K., Wang, Y., Hutchings, J. W., Delhomme, O., Kommalapati, R. R., Herckes, P.,
717 Wornat, M. J., and Valsaraj, K. T.: Processing of atmospheric polycyclic aromatic hydrocarbons by fog in an urban
718 environment, *Journal of Environmental Monitoring*, 14, 2566-2579, 10.1039/C2EM30336A, 2012.

719 Gioda, A., Mayol-Bracero, O. L., Scatena, F. N., Weathers, K. C., Mateus, V. L., and McDowell, W. H.: Chemical
720 constituents in clouds and rainwater in the Puerto Rican rainforest: Potential sources and seasonal drivers, *Atmos.*
721 *Environ.*, 68, 208-220, <https://doi.org/10.1016/j.atmosenv.2012.11.017>, 2013.

722 Gioda, A., Reyes-Rodríguez, G. J., Santos-Figueroa, G., Collett Jr, J. L., Decesari, S., Ramos, M. d. C. K. V.,
723 Bezerra Netto, H. J. C., de Aquino Neto, F. R., and Mayol-Bracero, O. L.: Speciation of water-soluble inorganic,
724 organic, and total nitrogen in a background marine environment: Cloud water, rainwater, and aerosol particles,
725 *Journal of Geophys. Res.: Atmos.*, 116, <https://doi.org/10.1029/2010JD015010>, 2011.

726 Guo, J., Wang, Y., Shen, X., Wang, Z., Lee, T., Wang, X., Li, P., Sun, M., Collett Jr, J. L., Wang, W., and Wang,
727 T.: Characterization of cloud water chemistry at Mount Tai, China: Seasonal variation, anthropogenic impact, and
728 cloud processing, *Atmos. Environ.*, 60, 467-476, <http://dx.doi.org/10.1016/j.atmosenv.2012.07.016>, 2012.

729 Guyot, G., Gourbeyre, C., Febvre, G., Shcherbakov, V., Burnet, F., Dupont, J. C., Sellegri, K., and Jourdan, O.:
730 Quantitative evaluation of seven optical sensors for cloud microphysical measurements at the Puy-de-Dôme
731 Observatory, France, *Atmos. Meas. Tech.*, 8, 4347-4367, 10.5194/amt-8-4347-2015, 2015.

732 Herckes, P., Valsaraj, K. T., and Collett Jr, J. L.: A review of observations of organic matter in fogs and clouds:
733 Origin, processing and fate, *Atmos. Res.*, 132–133, 434-449, 10.1016/j.atmosres.2013.06.005, 2013.

734 Herckes, P., Hannigan, M. P., Trenary, L., Lee, T., and Collett Jr, J. L.: Organic compounds in radiation fogs in
735 Davis (California), *Atmos. Res.*, 64, 99-108, 10.1016/s0169-8095(02)00083-2, 2002.

736 Herrmann, H., Schaefer, T., Tilgner, A., Styler, S. A., Weller, C., Teich, M., and Otto, T.: Tropospheric aqueous-
737 phase chemistry: Kinetics, mechanisms, and its coupling to a changing gas phase, *Chem. Rev.*, 115, 4259-4334,
738 10.1021/cr500447k, 2015.

739 Hoffmann, M. R.: On the kinetics and mechanism of oxidation of aquated sulfur dioxide by ozone, *Atmos.*
740 *Environ.*, 20, 1145-1154, 10.1016/0004-6981(86)90147-2, 1986.

741 Hu, W., Niu, H., Murata, K., Wu, Z., Hu, M., Kojima, T., and Zhang, D.: Bacteria in atmospheric waters: Detection,
742 characteristics and implications, *Atmos. Environ.*, 179, 201-221, <https://doi.org/10.1016/j.atmosenv.2018.02.026>,
743 2018.

744 Hutchings, J., Robinson, M., McIlwraith, H., Triplett Kingston, J., and Herckes, P.: The chemistry of intercepted
745 clouds in Northern Arizona during the North American monsoon season, *Water, Air, and Soil Poll.*, 199, 191-202,
746 10.1007/s11270-008-9871-0, 2009.

747 Joly, M., Amato, P., Deguillaume, L., Monier, M., Hoose, C., and Delort, A. M.: Quantification of ice nuclei active
748 at near 0 °C temperatures in low-altitude clouds at the Puy de Dôme atmospheric station, *Atmos. Chem. Phys.*, 14,
749 8185-8195, 10.5194/acp-14-8185-2014, 2014.

750 Kagawa, M., Katsuta, N., and Ishizaka, Y.: Chemical characteristics of cloud water and sulfate production under
751 excess hydrogen peroxide in a high mountainous region of central Japan, *Water, Air, & Soil Pollution*, 232, 177,
752 10.1007/s11270-021-05099-y, 2021.

753 Krusiz, C., Berner, A., and Brandner, B.: A cloud water sampler for high wind speeds, *Proceedings of the*
754 *EUROTRAC Symposium 1992* SPB Academic Publishing by, 1993, 523-525,

755 Lamkaddam, H., Dommen, J., Ranjithkumar, A., Gordon, H., Wehrle, G., Krechmer, J., Majluf, F., Salionov, D.,
756 Schmale, J., Bjelić, S., Carslaw, K. S., El Haddad, I., and Baltensperger, U.: Large contribution to secondary
757 organic aerosol from isoprene cloud chemistry, *Science Advances*, 7, eabe2952, doi:10.1126/sciadv.abe2952,
758 2021.

759 Laskin, A., Laskin, J., and Nizkorodov, S. A.: Chemistry of atmospheric brown carbon, *Chem. Rev.*, 115, 4335-
760 4382, 10.1021/cr5006167, 2015.

761 Lawrence, C. E., Casson, P., Brandt, R., Schwab, J. J., Dukett, J. E., Snyder, P., Yerger, E., Kelting, D.,
762 VandenBoer, T. C., and Lance, S.: Long-term monitoring of cloud water chemistry at Whiteface Mountain: the
763 emergence of a new chemical regime, *Atmos. Chem. Phys.*, 23, 1619-1639, 10.5194/acp-23-1619-2023, 2023.

764 Lebedev, A. T., Polyakova, O. V., Mazur, D. M., Artaev, V. B., Canet, I., Lallement, A., Väitilingom, M.,
765 Deguillaume, L., and Delort, A. M.: Detection of semi-volatile compounds in cloud waters by GC×GC-TOF-MS.
766 Evidence of phenols and phthalates as priority pollutants, *Environ. Poll.*, 241, 616-625,
767 <https://doi.org/10.1016/j.envpol.2018.05.089>, 2018.

768 Li, J., Wang, X., Chen, J., Zhu, C., Li, W., Li, C., Liu, L., Xu, C., Wen, L., Xue, L., Wang, W., Ding, A., and
769 Herrmann, H.: Chemical composition and droplet size distribution of cloud at the summit of Mount Tai, China,
770 *Atmos. Chem. Phys.*, 17, 9885-9896, 10.5194/acp-17-9885-2017, 2017.

771 Li, P. H., Wang, Y., Li, Y.-H., Wang, Z. F., Zhang, H. Y., Xu, P. J., and Wang, W. X.: Characterization of
772 polycyclic aromatic hydrocarbons deposition in PM_{2.5} and cloud/fog water at Mount Taishan (China), *Atmos.*
773 *Environ.*, 44, 1996-2003, 10.1016/j.atmosenv.2010.02.031, 2010.

774 Li, T., Wang, Z., Wang, Y., Wu, C., Liang, Y., Xia, M., Yu, C., Yun, H., Wang, W., Wang, Y., Guo, J., Herrmann,
775 H., and Wang, T.: Chemical characteristics of cloud water and the impacts on aerosol properties at a subtropical
776 mountain site in Hong Kong SAR, *Atmos. Chem. Phys.*, 20, 391-407, 10.5194/acp-20-391-2020, 2020.

777 Liu, Y., Lim, C. K., Shen, Z., Lee, P. K. H., and Nah, T.: Effects of pH and light exposure on the survival of
778 bacteria and their ability to biodegrade organic compounds in clouds: implications for microbial activity in acidic
779 cloud water, *Atmos. Chem. Phys.*, 23, 1731-1747, 10.5194/acp-23-1731-2023, 2023.

780 Löflund, M., Kasper-Giebl, A., Schuster, B., Giebl, H., Hitzenberger, R., and Puxbaum, H.: Formic, acetic, oxalic,
781 malonic and succinic acid concentrations and their contribution to organic carbon in cloud water, *Atmos. Environ.*,
782 36, 1553-1558, 10.1016/s1352-2310(01)00573-8, 2002.

783 Lüttke, J., Levsen, K., Acker, K., Wieprecht, W., and Möller, D.: Phenols and nitrated phenols in clouds at mount
784 Brocken, *International Journal of Environ. Anal. Chem.*, 74, 69-89, 10.1080/03067319908031417, 1999.

785 MacDonald, A. B., Dadashazar, H., Chuang, P. Y., Crosbie, E., Wang, H., Wang, Z., Jonsson, H. H., Flagan, R.
786 C., Seinfeld, J. H., and Sorooshian, A.: Characteristic vertical profiles of cloud water composition in marine
787 stratocumulus clouds and relationships with precipitation, *Journal of Geophys. Res.: Atmos.*, 123, 3704-3723,
788 <https://doi.org/10.1002/2017JD027900>, 2018.

789 Marinoni, A., Laj, P., Sellegri, K., and Mailhot, G.: Cloud chemistry at the puy de Dôme: variability and
790 relationships with environmental factors, *Atmos. Chem. Phys.*, 4, 715-728, 10.5194/acp-4-715-2004, 2004.

791 Marinoni, A., Parazols, M., Brigante, M., Deguillaume, L., Amato, P., Delort, A.-M., Laj, P., and Mailhot, G.:
792 Hydrogen peroxide in natural cloud water: Sources and photoreactivity, *Atmos. Res.*, 101, 256-263,
793 10.1016/j.atmosres.2011.02.013, 2011.

794 Marple, V. A. and Willeke, K.: Impactor design, *Atmos. Environ.* (1967), 10, 891-896,
795 [https://doi.org/10.1016/0004-6981\(76\)90144-X](https://doi.org/10.1016/0004-6981(76)90144-X), 1976.

796 Munger, J. W., Jacob, D. J., Waldman, J. M., and Hoffmann, M. R.: Fogwater chemistry in an urban atmosphere,
797 *Journal of Geophys. Res.*, 88, 5109-5121, <https://doi.org/10.1029/JC088iC09p05109>, 1983.

798 Munger, J. W., Jacob, D. J., Daube, B. C., Horowitz, L. W., Keene, W. C., and Heikes, B. G.: Formaldehyde,
799 glyoxal, and methylglyoxal in air and cloudwater at a rural mountain site in central Virginia, *Journal of Geophys.*
800 *Res.*, 100, 9325-9333, 10.1029/95jd00508, 1995.

801 Pailler, L., Wirgot, N., Joly, M., Renard, P., Mouchel-Vallon, C., Bianco, A., Leriche, M., Sancelme, M., Job, A.,
802 Patryl, L., Armand, P., Delort, A.-M., Chaumerliac, N., and Deguillaume, L.: Assessing the efficiency of water-
803 soluble organic compound biodegradation in clouds under various environmental conditions, *Environ. Sci.:*
804 *Atmos.*, 3, 731-748, 10.1039/D2EA00153E, 2023.

805 Pye, H. O. T., Nenes, A., Alexander, B., Ault, A. P., Barth, M. C., Clegg, S. L., Collett Jr, J. L., Fahey, K. M.,
806 Hennigan, C. J., Herrmann, H., Kanakidou, M., Kelly, J. T., Ku, I. T., McNeill, V. F., Riemer, N., Schaefer, T.,
807 Shi, G., Tilgner, A., Walker, J. T., Wang, T., Weber, R., Xing, J., Zaveri, R. A., and Zuend, A.: The acidity of
808 atmospheric particles and clouds, *Atmos. Chem. Phys.*, 20, 4809-4888, 10.5194/acp-20-4809-2020, 2020.

809 Renard, P., Bianco, A., Baray, J.-L., Bridoux, M., Delort, A.-M., and Deguillaume, L.: Classification of clouds
810 sampled at the puy de Dôme station (France) based on chemical measurements and air mass history matrices,
811 *Atmosphere*, 11, 732, <https://doi.org/10.3390/atmos11070732>, 2020.

812 Renard, P., Brissy, M., Rossi, F., Leremboure, M., Jaber, S., Baray, J. L., Bianco, A., Delort, A. M., and
813 Deguillaume, L.: Free amino acid quantification in cloud water at the Puy de Dôme station (France), *Atmos. Chem.*
814 *Phys.*, 22, 2467-2486, 10.5194/acp-22-2467-2022, 2022.

815 Roman, P., Polkowska, Ż., and Namieśnik, J.: Sampling procedures in studies of cloud water composition: a
816 review, *Critical Reviews in Environmental Science and Technology*, 43, 1517-1555,
817 10.1080/10643389.2011.647794, 2013.

818 Rossi, F., Péguilhan, R., Turgeon, N., Veillette, M., Baray, J.-L., Deguillaume, L., Amato, P., and Duchaine, C.:
819 Quantification of antibiotic resistance genes (ARGs) in clouds at a mountain site (puy de Dôme, central France),
820 *STOTEN*, 865, 161264, <https://doi.org/10.1016/j.scitotenv.2022.161264>, 2023.

821 Schell, D., Georgii, H. W., Maser, R., Jaeschke, W., Arends, B. G., Kos, G. P. A., Winkler, P., Schneider, T.,
822 Berner, A., and Krusiz, C.: Intercomparison of fog water samplers, *Tellus B*, 44, 612-631,
823 <https://doi.org/10.1034/j.1600-0889.1992.t01-1-00014.x>, 1992.

824 Schurman, M. I., Boris, A., Desyaterik, Y., and Collett, J. J. L.: Aqueous secondary organic aerosol formation in
825 ambient cloud water photo-oxidations, *AAQR*, 18, 15-25, 10.4209/aaqr.2017.01.0029, 2018.

826 Skarżyńska, K., Polkowska, Ż., and Namieśnik, J.: Sampling of atmospheric precipitation and deposits for analysis
827 of atmospheric pollution, *Journal of Automated Methods and Management in Chemistry*, 2006, 026908,
828 10.1155/JAMMC/2006/26908, 2006.

829 Sun, W., Fu, Y., Zhang, G., Yang, Y., Jiang, F., Lian, X., Jiang, B., Liao, Y., Bi, X., Chen, D., Chen, J., Wang, X.,
830 Ou, J., Peng, P., and Sheng, G.: Measurement report: Molecular characteristics of cloud water in southern China
831 and insights into aqueous-phase processes from Fourier transform ion cyclotron resonance mass spectrometry,
832 *Atmos. Chem. Phys.*, 21, 16631-16644, 10.5194/acp-21-16631-2021, 2021.

833 Sun, X., Wang, Y., Li, H., Yang, X., Sun, L., Wang, X., Wang, T., and Wang, W.: Organic acids in cloud water
834 and rainwater at a mountain site in acid rain areas of South China, *Environmental Science and Pollution Research*,
835 23, 9529-9539, 10.1007/s11356-016-6038-1, 2016.

836 Tenberken-Pötzsch, B., Schwikowski, M., and Gäggeler, H. W.: A method to sample and separate ice crystals and
837 supercooled cloud droplets in mixed phased clouds for subsequent chemical analysis, *Atmos. Environ.*, 34, 3629-
838 3633, [https://doi.org/10.1016/S1352-2310\(00\)00140-0](https://doi.org/10.1016/S1352-2310(00)00140-0), 2000.

839 Triesch, N., van Pinxteren, M., Engel, A., and Herrmann, H.: Concerted measurements of free amino acids at the
840 Cape Verde Islands: High enrichments in submicron sea spray aerosol particles and cloud droplets, *Atmos. Chem.*
841 *Phys.*, 21, 163-181, 10.5194/acp-21-163-2021, 2021.

842 Vaïtilingom, M., Deguillaume, L., Vinatier, V., Sancelme, M., Amato, P., Chaumerliac, N., and Delort, A.-M.:
843 Potential impact of microbial activity on the oxidant capacity and organic carbon budget in clouds, *PNAS*, 110,
844 559-564, 10.1073/pnas.1205743110, 2013.

845 Vaïtilingom, M., Attard, E., Gaiani, N., Sancelme, M., Deguillaume, L., Flossmann, A. I., Amato, P., and Delort,
846 A.-M.: Long-term features of cloud microbiology at the puy de Dôme (France), *Atmos. Environ.*, 56, 88-100,
847 10.1016/j.atmosenv.2012.03.072, 2012.

848 van Pinxteren, D., Neusüß, C., and Herrmann, H.: On the abundance and source contributions of dicarboxylic acids
849 in size-resolved aerosol particles at continental sites in central Europe, *Atmos. Chem. Phys.*, 14, 3913-3928,
850 10.5194/acp-14-3913-2014, 2014.

851 van Pinxteren, D., Fomba, K. W., Mertes, S., Müller, K., Spindler, G., Schneider, J., Lee, T., Collett, J. L., and
852 Herrmann, H.: Cloud water composition during HCCT-2010: Scavenging efficiencies, solute concentrations, and
853 droplet size dependence of inorganic ions and dissolved organic carbon, *Atmos. Chem. Phys.*, 16, 3185-3205,
854 10.5194/acp-16-3185-2016, 2016.

855 van Pinxteren, D., Plewka, A., Hofmann, D., Müller, K., Kramberger, H., Svrčina, B., Bächmann, K., Jaeschke,
856 W., Mertes, S., Collett Jr, J. L., and Herrmann, H.: Schmücke hill cap cloud and valley stations aerosol
857 characterisation during FEBUKO (II): Organic compounds, *Atmos. Environ.*, 39, 4305-4320,
858 10.1016/j.atmosenv.2005.02.014, 2005.

859 van Pinxteren, M., Fomba, K. W., Triesch, N., Stolle, C., Wurl, O., Bahlmann, E., Gong, X., Voigtländer, J., Wex,
860 H., Robinson, T. B., Barthel, S., Zeppenfeld, S., Hoffmann, E. H., Roveretto, M., Li, C., Grosselin, B., Daële, V.,
861 Senf, F., van Pinxteren, D., Manzi, M., Zabalegui, N., Frka, S., Gašparović, B., Pereira, R., Li, T., Wen, L., Li, J.,
862 Zhu, C., Chen, H., Chen, J., Fiedler, B., von Tümpling, W., Read, K. A., Punjabi, S., Lewis, A. C., Hopkins, J. R.,
863 Carpenter, L. J., Peeken, I., Rixen, T., Schulz-Bull, D., Monge, M. E., Mellouki, A., George, C., Stratmann, F.,
864 and Herrmann, H.: Marine organic matter in the remote environment of the Cape Verde islands – an introduction
865 and overview to the MarParCloud campaign, *Atmos. Chem. Phys.*, 20, 6921-6951, 10.5194/acp-20-6921-2020,
866 2020.

867 Waldman, J. M., Munger, J. W., J., J. D., and Hoffmann, M. R.: Chemical characterization of stratus cloudwater
868 and its role as a vector for pollutant deposition in a Los Angeles pine forest, *Tellus B*, 37B, 91-108,
869 <https://doi.org/10.1111/j.1600-0889.1985.tb00058.x>, 1985.

870 Wang, M., Perroux, H., Fleuret, J., Bianco, A., Bouvier, L., Colomb, A., Borbon, A., and Deguillaume, L.:
871 Anthropogenic and biogenic hydrophobic VOCs detected in clouds at the puy de Dôme station using Stir Bar
872 Sorptive Extraction: Deviation from the Henry's law prediction, *Atmos. Res.*, 237, 104844,
873 <https://doi.org/10.1016/j.atmosres.2020.104844>, 2020.

- 874 Wei, M., Xu, C., Chen, J., Zhu, C., Li, J., and Lv, G.: Characteristics of bacterial community in cloud water at Mt
875 Tai: similarity and disparity under polluted and non-polluted cloud episodes, *Atmos. Chem. Phys.*, 17, 5253-5270,
876 10.5194/acp-17-5253-2017, 2017.
- 877 Wieprecht, W., Acker, K., Mertes, S., Collett, J., Jaeschke, W., Brüggemann, E., Möller, D., and Herrmann, H.:
878 Cloud physics and cloud water sampler comparison during FEBUKO, *Atmos. Environ.*, 39, 4267-4277,
879 <https://doi.org/10.1016/j.atmosenv.2005.02.012>, 2005.
- 880 Wright, L. P., Zhang, L., Cheng, I., Aherne, J., and Wentworth, G. R.: Impacts and effects indicators of
881 atmospheric deposition of major pollutants to various ecosystems - a review, *AAQR*, 18, 1953-1992,
882 10.4209/aaqr.2018.03.0107, 2018.
- 883 Xu, C., Wei, M., Chen, J., Sui, X., Zhu, C., Li, J., Zheng, L., Sui, G., Li, W., Wang, W., Zhang, Q., and Mellouki,
884 A.: Investigation of diverse bacteria in cloud water at Mt. Tai, China, *STOTEN*, 580, 258-265,
885 <http://dx.doi.org/10.1016/j.scitotenv.2016.12.081>, 2017.
- 886 Zhao, Y., Hallar, A. G., and Mazzoleni, L. R.: Atmospheric organic matter in clouds: exact masses and molecular
887 formula identification using ultrahigh-resolution FT-ICR mass spectrometry, *Atmos. Chem. Phys.*, 13, 12343-
888 12362, 10.5194/acp-13-12343-2013, 2013.